Graduate School ETD Form 9
(Revised 12/07)

PURDUE UNIVERSITY
GRADUATE SCHOOL
Thesis/Dissertation Acceptance

This is to certify that the thesis/dissertation prepared

By Keith Rennier

Entitled THE ROLE OF DAP-KINASE IN MODULATING VASCULAR ENDOTHELIAL CELL FUNCTION UNDER FLUID SHEAR STRESS

For the degree of Master of Science in Biomedical Engineering

Is approved by the final examining committee:

Chair	
Julie Ying Hui Ji	Julie Ying Hui Ji
Hiroki Yokota	Hiroki Yokota
Jiliang Li	Jiliang Li

To the best of my knowledge and as understood by the student in the *Research Integrity and Copyright Disclaimer (Graduate School Form 20)*, this thesis/dissertation adheres to the provisions of Purdue University's "Policy on Integrity in Research" and the use of copyrighted material.

Approved by Major Professor(s): Julie Ying Hui Ji

Approved by: Ed Berbari 4/16/10
Head of the Graduate Program Date

Graduate School Form 20
(Revised 1/10)

PURDUE UNIVERSITY
GRADUATE SCHOOL

Research Integrity and Copyright Disclaimer

Title of Thesis/Dissertation:

THE ROLE OF DAP-KINASE IN MODULATING VASCULAR ENDOTHELIAL CELL FUNCTION UNDER FLUID SHEAR STRESS

For the degree of Master of Science in Biomedical Engineering

I certify that in the preparation of this thesis, I have observed the provisions of *Purdue University Teaching, Research, and Outreach Policy on Research Misconduct (VIII.3.1)*, October 1, 2008.*

Further, I certify that this work is free of plagiarism and all materials appearing in this thesis/dissertation have been properly quoted and attributed.

I certify that all copyrighted material incorporated into this thesis/dissertation is in compliance with the United States' copyright law and that I have received written permission from the copyright owners for my use of their work, which is beyond the scope of the law. I agree to indemnify and save harmless Purdue University from any and all claims that may be asserted or that may arise from any copyright violation.

Keith Rennier

Printed Name and Signature of Candidate

04/15/2010

Date (month/day/year)

*Located at http://www.purdue.edu/policies/pages/teach_res_outreach/viii_3_1.html

THE ROLE OF DAP-KINASE IN MODULATING VASCULAR ENDOTHELIAL CELL FUNCTION UNDER FLUID SHEAR STRESS

A Thesis
Submitted to the Faculty
of
Purdue University
by
Keith Rennier

In Partial Fulfillment of the
Requirements for the Degree
of
Master of Science in Biomedical Engineering

May 2010
Purdue University
Indianapolis, Indiana

ACKNOWLEDGMENTS

I would like to gratefully thank and acknowledge my thesis advisor, Dr. Julie Ying Hui Ji, for her mentoring and support along the way, from start to finish. Also, I am appreciative of her giving me the chance to be a part of relevant research and sharing her time and expertise.

I would like to thank my advisory committee members, Dr. Hiroki Yokota, and Dr. Jiliang Li, for their time and support during the research process.

I would also like to give a special thanks to all my family and friends for their endless support and patience.

Lastly, I offer my best regards and blessings to all of those who supported me in any respect during the completion of this thesis project.

TABLE OF CONTENTS

Page

LIST OF TABLES

LIST OF FIGURES

ABSTRACT

Rennier, Keith. M.S.B.M.E., Purdue University, May 2010. The Role of DAP-Kinase in Modulating Vascular Endothelial Cell Function under Fluid Shear Stress. Major Professor: Julie Ying Hui Ji.

Atherosclerosis preferentially develops in vascular regions of low or disturbed flow and high spatial gradients. Endothelial cells that line the vessel walls actively participate in translating mechanical stimuli, shear stress due to fluid flow, into intracellular signals to regulate cellular activities. Atherosclerosis is a chronic disease. During its development, a cascade of inflammatory signals alters the arterial endothelial homeostatic functions.

Death-associated protein (DAP) kinase and its correlated pathway have been associated with cell apoptosis, turnover, and cytoskeleton remodeling in cellular networks, ultimately leading to changes in cell motility and vascular wall permeability. DAP-kinase is also highly regulated by inflammatory triggers such as TNF-α. This thesis investigates DAP-kinase modulation due to shear stress, and the role of DAP-kinase activity in endothelial responses toward applied shear stress. Using bovine aortic endothelial cells (BAEC), DAP-kinase expression is demonstrated in both sheared (10 dynes/cm^2) and static conditions. Overall DAPK expression increased with extended shearing, while the presence of phosphorylated DAPK decreased with applied shear stress, as demonstrated in Western blot analysis.

In correlation, DAPK RNA expression profiles were explored to understand pre-translational behavior and to understand just how shear stress influences DAPK expression over time. There is a temporal increase in DAPK mRNA, occurring at earlier time points when compared to DAPK protein expression, displaying the precedence of mRNA expression leading to increased translation into protein.

From our apoptosis assay results, shear stress reduces apoptotic and late stage/necrotic cell fractions. The exposure of shear stress potentially plays a role in inhibiting apoptosis activation and TNF-α induced death cascade.

Overall, the apoptosis activity influenced by shear further exhibits a possible connection between shear stress and apoptosis inhibition. The shear stress ultimately decreases overall apoptosis, while DAPK expression is increased. Therefore, DAPK may have a function in other possible mechano-transduction cascades, when endothelial cells are exposed to constant shear. Our data suggests shear stress modulation of DAP-kinase expression and activity, and the potential crosstalk of mechano-transduction and DAPK-apoptosis pathway, may lead to further understanding the responsibility of DAPK in endothelial cell function.

1. INTRODUCTION

The thesis will begin with some background on the cardiovascular biology involved, as well as the engineering principles applied for the research. The specific thesis objectives will be outlined, followed by the research methods, results, and overall conclusions. Finally, the significance of the thesis project and future directions will be discussed.

1.1 Understanding the Artery

It is important to understand basic biology of the cardiovascular system to understand the research direction of this thesis project. The arterial blood vessel wall is composed of three different layers. The outermost layer, the adventitia, is made up of collection of connective tissue and interwoven thick collagen fibers, ultimately connecting blood vessels to external tissue networks. The central tissue layer, or media, contains smooth muscle cells within a network of collagen and externally protected by a layer of elastic tissue, also known as the external elastic lamina. Within the media layer, the smooth muscle cells and elastin fibers align circumferentially in order to provide mechanical integrity to the blood vessel wall. Lastly, the innermost layer, or intima, is composed of a layer of endothelial cells backed by a layer of elastic connective tissue, or internal elastic lamina. The intima layer is the tissue interface with the blood flow within the cardiovascular system [1]. Figure 1.1 shows the sections of each of the three different blood vessel layers.

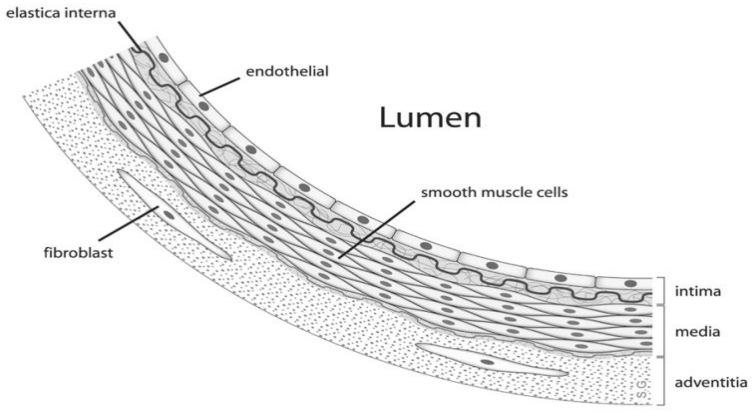

Figure 1.1 Anatomy of the arterial wall [2]

The hemodynamic forces generated by blood flow, exert both pressure and shear stress to the luminal lining of the artery. The applied forces create pressure in the normal direction due to cyclic stretch and intercellular signaling due to tangential shearing due to axial fluid flow. The hemodynamic forces within the vessel wall are shown in Figure 1.2 [3]. The endothelial cells that line the arterial wall are exposed to both the biochemical environmental conditions and mechanical stimuli introduced by the blood flow and in turn engage in intercellular signaling based on these signals.

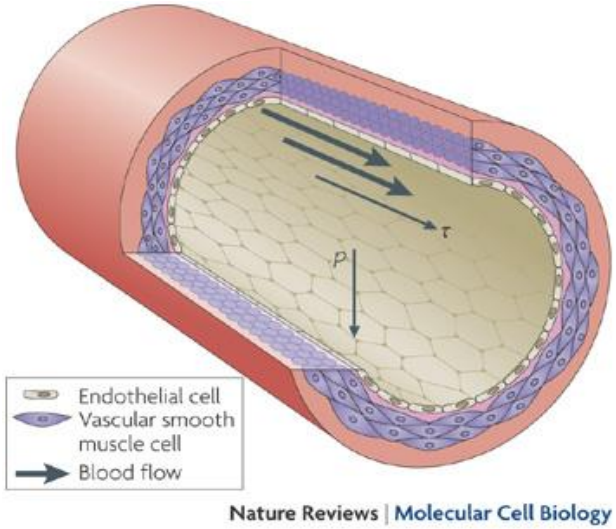

Figure 1.2 Mechanical forces acting on vessel wall

The arterial endothelial cells respond to mechanical stimuli, such as shear stress, with intracellular signals in the cardiovascular system. For example, shear stress influences endothelial cell wall remodeling through the production of growth-promoting and growth-inhibiting signaling molecules. Additionally, the endothelial cells control hemostasis and thrombosis by providing pro-coagulant, anti-coagulant, and fibrinolytic mediators. By releasing chemotactic and immune response surface molecules, the cells control inflammatory interactions that may occur within arterial system as well. Likewise, they will release vasodilators and vasoconstrictors in order to regulate smooth muscle cell contraction [4]. Collectively, the arterial endothelial cells play a substantial role in efficient functioning of cardiovascular system. Endothelial cells are actively participating in all homeostatic activities of the vascular wall, and as a result, impairment with the endothelial cells could lead to possible diseased states, by increasing the likelihood for positive atherogenic or thrombotic occurrences [5].

The main focus of this thesis will be to understand cellular mechano-transduction of the arterial endothelial cells. The overall goal of this project is to understand the intracellular signaling pathways of endothelial cells that are initiated and regulated by applied shear stress. Understanding endothelial mechano-transduction has become an important target for cardiovascular research because endothelial dysfunction can lead to cardiovascular diseases, such as atherosclerosis.

1.2 Disease Progression: Atherosclerosis

Atherosclerosis is a chronic disease that affects the arterial walls of the cardiovascular system, resulting in inflammation and reduced blood flow. With this condition, plaque builds up within the artery walls, causing a narrowing of the blood vessels. The arterial damage may occur overtime from a number of possible factors such as: a diet high in cholesterols and triglycerides, high blood pressure and/or stress, smoking, diabetes, and even genetics can play a role in the development of atherosclerosis [6].

Initially, the arterial plaque starts to build up due to damage that has occurred to the endothelium of the artery, such as the inflammatory response to endothelial damage or other immune responses. Specifically, atherosclerosis starts with the excess accumulation of cholesterol, low density lipoprotein (LDL), and fats in the sub-endothelial space, or fatty streaks. As the disease progresses with continued deposits of excess cholesterol, fatty streaks develop into plaques, and atherosclerotic plaques begin to restrict blood flow. This is a chronic inflammatory condition of the endothelium. Eventually, plaques develop into a thrombotic pool covered by a fibrous cap. Breakage of this fibrous cap leads to immediate blot clot, resulting in heart attack or stroke [7, 8].

One of the major disease conditions that develop from the spread of atherosclerosis is coronary or peripheral arterial disease. In coronary arterial disease, blockage has developed in major arteries supplying blood to heart, and in peripheral arterial disease, blockage effect arteries that supply blood other major organs of the body, in the peripheral. Over 12 million patients are in the progressing stages of coronary artery disease, with one in five deaths occurring from cardiovascular disease in the United States alone [9]. Atherosclerosis is one of the leading causes of death in developed countries, with a substantially large patient population. There is a tremendous need for identification of drug targets, improved biological therapeutics or medical devices for the prevention and treatment of atherosclerosis.

1.3 Disease Mechanism of Atherosclerosis

Atherosclerosis was originally thought to be degenerative, just a consequence of aging. After extensive research, it was shown to have a complex progression from a cycle of cellular events.

Initially, blood transports excessive amount of fat and/or lipoproteins due to diet or other factors. Low density lipoproteins (LDLs) are the “bad” cholesterol that is at the root of atherosclerotic development. Overload of LDLs results in a high absorption into

the arterial walls, along with retention of these molecules, creating what is known as a fatty streak in the arteries. With the LDLs trapped in the wall, they form connective fibers in the extracellular matrix of the arteries. The LDLs are then oxidized by the surrounding microenvironment, directing monocytes to the arterial entrapment location. From further oxidation, the LDL structure is altered, resulting in the loss of recognition of its receptors. This leads to the surrounding cell receptors gaining the ability to bind the low-density lipoproteins, without discrimination of cholesterol content, in order to uptake into the arterial cells [10].

As a result, this LDL uptake allows for a large increase in cholesterol within the arterial cells creating lesions in the artery. The development of lesions triggers an immune response to address the arterial damage. Unfortunately, the increase of cellular LDL concentration results in rejection of neutrophils, due to the toxic composition of the LDL molecules. This is a chronic inflammatory condition of the endothelium, and as atherosclerosis continues to develop, fatty streaks develop in to plaque deposits, and inflammation is accelerated at the damaged location. Sites of highly concentrated cholesterol will continue to grow and expand into arterial lesion. See Figure 1.3.

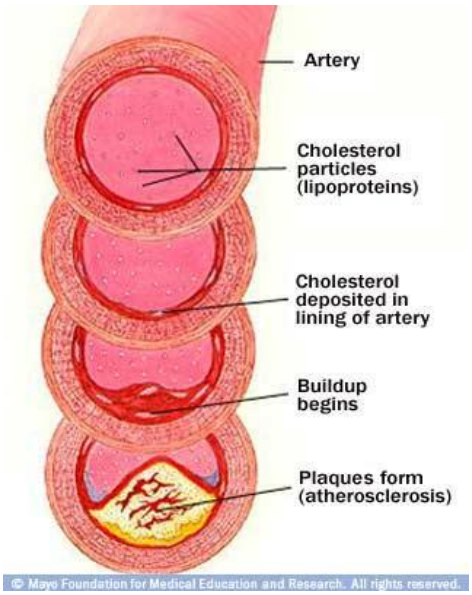

Figure 1.3 Disease progression decreasing blood flow [11]

Macrophages that move into atherosclerotic plaques develop into foam cells as they continue to accumulate LDL, and smooth muscle cells migrate over endothelial plaques and begin to produce extracellular matrix proteins that form a fibrous cap which covers a diseased and inflammatory core that is highly thrombotic. Eventually, the arterial plaque that has aggregated at these lesion sites may rupture at sites of structural/mechanical weakness [12]. Lesion ruptures will illicit additional immune response and induces an increase in cellular/monocytes tissue factor, which is a strong coagulant for the arterial cells. The introduction of this tissue factor to the blood will initiate thrombosis at the rupture site [10]. Thrombosis starts a blood clotting cascade, which will lead to complete blockage of the artery, as is the case during a heart attack, if clotting occurs at the coronary artery or stroke if clotting occurs in vessels of the brain.

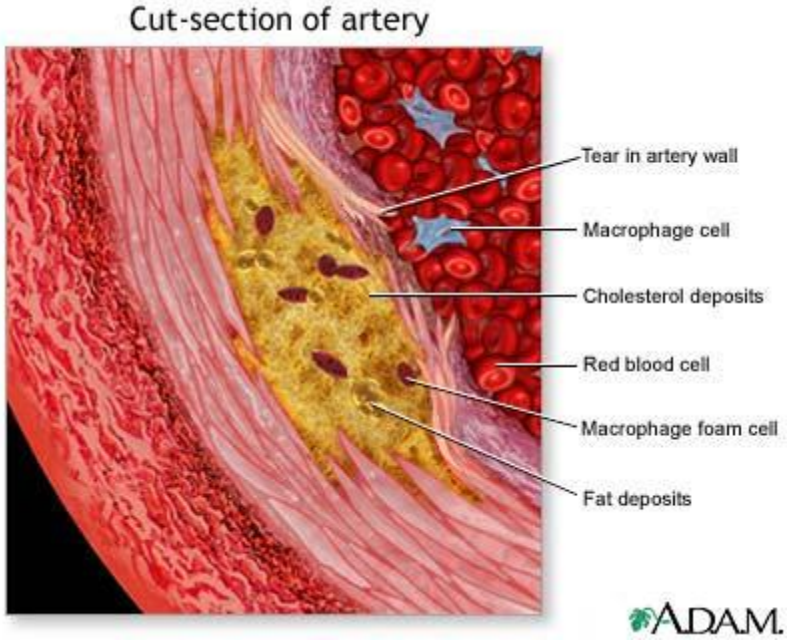

Figure 1.4 Arterial lesion damage and progression [13]

Overtime, atherosclerosis will progress as a narrowing of arteries due to plaque formation, to slow blood flow or reduce cardiac efficiency. This arterial blockage can potentially lead to multiple health problems, such as heart failure and stroke [7, 10].

Over the past decade, a research focus has been on developing therapeutic strategies, as well as understanding the roles of important cardiovascular factors [14]. This project aims to improve the understanding of the disease mechanisms in order to better prevent the development of atherosclerosis.

1.4 Hemodynamics and Shear Stress

At the cellular level, there are many factors that control the various functions of the artery. Cell signaling can be initiated by a number of different stimuli, such as chemical interactions, potential gradients, or mechanical shear and stretch. Shear stress due to hemodynamic flow within an artery directly affects the endothelial cells lining the blood vessel wall. Endothelial cells will respond in different ways depending on the type of flow applied, transferring signals throughout the system to facilitate specific functions. Shear stress, depending on the respective flow pattern, can induce cells to express different proteins to facilitate cell proliferation, apoptosis, cell motility, anti-pathogenesis, and pro-pathogenesis factors. Both morphological and functional changes occur continuously in order to maintain artery structure and function.

With such a dynamic structure, there is constant endothelial cell turnover within the artery. As a result, there are many different regulators of the system, in order to maintain cardiovascular efficiency and cell wall integrity. As blood flow shears the endothelial lining, the cell turnover can create the potential for trans-endothelial leakage of macromolecules, including low density lipoproteins [5]. This leakage susceptibility can allow for the progression of a cumulative condition, such as atherosclerosis. For the case of vascular failure, there is a breakdown in expression of specific protective molecules, and/or an up-regulation of certain pro-pathogenic molecules [15]. By understanding the system regulators and shear stress influences, it can lead to possible disease factors and prevention tactics for these conditions.

As previously discussed, atherosclerosis is a chronic inflammatory disease involving accumulation of multiple lipid, protein, immune system components, smooth muscle cells migration; resulting in fatty streaks and plaques in the arterial walls at the legion sites, whose rupture leads to thrombosis, heart attack, and possibly death. In the vasculature, atherosclerosis develops preferentially at branching points, and disturbed sections of the vascular tree where disturbed hemodynamic flow patterns exist. Disturbed flow is where endothelial cells can be exposed to low levels of shear stress, reversing or vortexing flow. On the other hand, atherosclerosis is less likely to develop in straight sections of vascular tree with more laminar flow pattern and higher levels of shear stress [8].

As for specific shear flow and comparing gene expression profiles in laminar versus disturbed flow, laminar flow has shown to up-regulate endothelial cell anti-inflammatory genes, where as disturbed flow has shown to down regulated these specific genes. Also, disturbed flow can allow for an increase in pro-inflammatory gene expression. Endothelial cell proliferation and cell death are increased by reciprocal flow patterns. Likewise, pulsatile shear flow has been shown to inhibit this cell turnover process. In reducing the cell wall activity, the progression of the arterial lesions will be inhibited, as seen in the straight sections of arteries exposed to laminar shear flow [5]. Arterial plaque and wall damage tend to develop in curved or branched regions, where shear stress is low and flow conditions are associated with a high spatial gradient. Consequently, the blood flow becomes disturbed and unsteady in the low sheared locations, obviously affecting endothelial cell function [7].

In reviewing the systematic development of arterial lesions, they have all been shown to have the same hemodynamic flow conditions, regardless of individual risk factors or lifestyle choices [5]. This leads to an insight that these specific regions are influenced by the shear stress, as well as other specific risk factors: the reduced anti-atherogenic factors and increase of pro-atherogenic factors at the respective lesion sites.

Thus, shear stress is an important regulator of endothelial cell functions, and plays an important role in mediating the development of atherosclerosis [8].

Further investigation of important molecular mechanisms in arterial endothelial cell function using shear stress and mechano-transduction studies, will help identify novel approaches to treating cardiovascular disease. Using mechano-transduction studies, molecular pathways influencing endothelial cell dysfunction can be fully understood. This knowledge will lead to the development of new drug targets, and more efficient techniques for disease prevention, detection, as well as treatment.

1.5 DAP-Kinase and Its Corresponding Cascades

In regulation of cellular pathways, protein kinases play a large role in modifying proteins and their respective functions. These kinases can affect target proteins in many different ways such as: changing enzymatic activity, location within the cell, protein-protein interactions, and further signal transduction processes within a cell. Specifically, protein kinase is an enzyme that chemically alters a protein by adding a phosphate group to the target substrate, also known as phosphorylation. In adding a phosphate to the substrate, this results in a functional modification to the directly affected protein. To phosphorylate substrate proteins, kinases will attach a phosphate group to one of the three amino acids with a free hydroxyl group: serine, threonine, or tyrosine. The substrate transformation can lead to signal transduction to other cellular processes, displaying the vital importance of protein kinases and their regulatory activities.

The protein kinases are highly regulated due to their role in various cellular processes, such as cell growth, motility, and death processes. The kinase activity is switched on and off by specific protein phosphorylation/dephosphorylation [16]. Protein kinases are activated through binding of specific activator/inhibitor proteins, particular cellular location, small molecule activators, and some are even auto-phosphorylated directly by the kinase.

Based on the importance of efficient kinase function, a disturbance in kinase activity regulation can lead to the altered signal transduction and a resulting development of particular diseases [17, 18].

Death-Associated Protein Kinase (DAPK) is a calcium/calmodulin regulated, serine/threonine kinase involved in a number of different cellular functions, required in order to maintain a balance between cell proliferation and death. Within the cell, DAPK is localized to cytoskeleton, where it can regulate and/or phosphorylate cytoskeletal proteins, such as actin microfilaments [19]. Due to its cytoskeleton involvement, DAPK can regulate cell adhesion, motility, and possible cell structure integrity or organization, all of which play a role in the programmed cell death processes, apoptosis.

This cytoskeleton-associated protein has been connected with cytokine activation of apoptosis, such as in the presence of Tissue Necrosis Factor – alpha (TNF-α). DAPK has shown pro-apoptotic effects by inactivating integrin β1, resulting in activation of the p53 apoptotic cascade and altering the extracellular matrix. Although DAPK is involved in apoptosis, its role in integrin modulation and cellular organization, due to cytoskeleton binding, also allows for DAPK to influence cell motility based on its inactivation of Cdc42 signaling cascade [20, 21].

DAPK protein structure is shown in Figure 1.5, including its various binding sites and domains. DAPK is a 160-kD protein with multiple catalytic and non-catalytic domains coming together to form the structure. There are 8 ankyrin repeats involved in mediating protein-protein interactions with DAPK. Also, DAPK contains binding sequence motifs, P-loops, a death domain, cytoskeleton binding motif, as well as a kinase catalytic domain [22, 23]. Specifically, the Ca2+/Calmodulin and the kinase domains are responsible regulating catalytic activities and recognizing specificities of substrate interaction. The rest of the molecular components of DAPK (P-loops, ankyrin repeats, and cytoskeleton and death domains) are involved in sub-cellular localization and protein interactions [24].

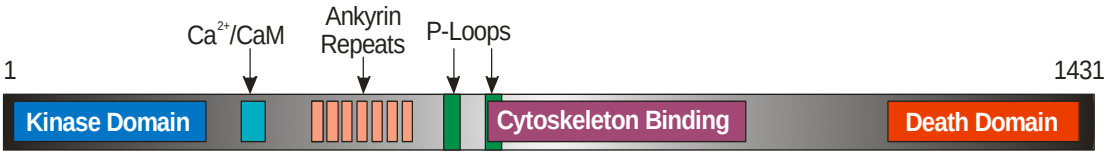

Figure 1.5 Schematic diagram of DAP-Kinase protein structure

In Table 1.1, the multiple phosphorylation sites influencing DAPK activity are described, along with the specific location sites within the protein molecule.

Table 1.1 Phosphorylation of DAPK influencing kinase activity

Phosphorylation Site	**Location of Phosphorylation**	**Mechanism of Action**	**Reference**
Phosphorylation due to p90 ribosomal S6 kinases (RSK) at Serine 239	Ca^{2+}/Calmodulin domain	Triggers suppression of pro-apoptotic function	[25]
Auto-phosphorylation at Serine 308	Ca^{2+}/Calmodulin domain	Influences cytokine apoptotic pathway; p53 dependent pathway	[26]
Extracellular Signal-Regulated Kinase (ERK) phosphorylation at Serine 735	In between Ankyrin repeats and the P-loop	Switches off the ERK-C/EBP-beta pathway, Up-regulating the cell turnover processes	[27]
Phosphorylation by SRC at Tyrosine 491/492	Within the 8 Ankyrin repeats	Stimulates intra-molecular interaction and inactivation	[28]
Dephosphorylated due to leukocyte common antigen-related (LAR) tyrosine phosphatase at Tyrsoine pY491/492	Within the 8 Ankyrin repeats	Induces the catalytic activity of DAPK, reducing cell adhesion and motility	[28]

DAP kinase is stimulated by increasing proliferative signals and calcium concentration and calmodulin activation. Specifically, DAPK operates upstream of $p19^{ARF}$ and p53 to induce apoptosis [29, 30]. DAPK-influenced cell death results in autophagic vesicle formation and membrane blebbing [31, 32].

From the list of possible phosphorylation sites in Table 1.1, the direction of potential thesis research linked to the auto-phosphorylation site at Serine 308, due to its involvement in apoptotic functions and Ca^{2+}/Calmodulin concentrations, correlating to the progression of atherosclerosis events. By studying both overall and phosphorylated DAPK, aortic endothelial cell experiments can give an idea of DAPK's overall cellular activity, and the connection between applied shear stress within a system.

Atherosclerotic lesions develop due to low shear stress exposure, reversing or vortexing flow, which facilitates fatty deposits and plaque formation. In regions of turbulent fluid flow, there is an increase in endothelial cell turnover, directly affecting the integrity of the vascular cell wall [15, 33]. A strong correlation is seen between cell turnover and trans-endothelial leakage of macromolecules, such as LDLs. Based on this correlation, these regions of disturbed flow are susceptible to cumulative arterial damage.

In correlation to lesion development, increased apoptotic cell death is shown to contribute to artery plaque formation, instability, rupture, and thrombus formations. DAPK is active in the apoptotic pathway and coincidentally up-regulated in atherosclerotic plaque regions [34]. The study of homeostatic vascular function will give insight into the diseased state of atherosclerosis, and the potential connection to DAPK due to its role in activating in the apoptotic pathway.

Endothelial cells respond using various signaling pathways in reaction to different kinds of applied stresses. Previous shear stress studies on endothelial cells have shown increased gene expression for various molecules implicated in atherosclerosis [35]. Yet, laminar hemodynamic flow has shown reduced endothelial cell turnover and increased anti-apoptotic expression, even in the presence of cytokine activation [36]. DAPK is a pro-apoptotic protein linked to pro inflammatory cytokines, such as TNF-α, that induce endothelial cell apoptosis [31]. This thesis project examines DAPK expression in effort to delineate its cellular functions in relation to the signal transduction pathway stimulated through shear stress. By investigating the communication between shear stress and

cytokines in regulating endothelial cell function, the cell signaling pathways can be better understood. Likewise, further understanding of cellular mechano-transduction, apoptosis pathways, and the role of DAPK in endothelial cells may lead to new approaches to atherosclerosis.

1.6 Thesis Objectives

The overall objective of this thesis project was to understand the endothelial mechano-transduction pathways involved in the development of atherosclerosis. More specifically, this project focused on analyzing the role of DAPK in sheared endothelial cells. There are two primarily goals or areas of focus in this project

First, this project aims to explore the expression of DAPK in endothelial cells under static or sheared conditions. The goal was to examine the influence of shear stress or hemodynamic simulation on DAPK expression over time.

In this research study, DAPK protein expression was examined both overall and phosphorylated, in cells exposed to extended shearing. Likewise, mRNA expression, in static and cells exposed to varying amounts of shear stress, was investigated using real-time RT-PCR analysis to determine the correlation between protein and mRNA levels. In order to follow the pre- and post-transcriptional activity of DAPK, the shear exposure periods were similarly conducted for both mRNA and protein samples, from 0 to 8 hours of applied shear.

Second, the connection between DAPK, apoptosis, which has DAPK in its activation cascade, and shear stress were investigated. Using Tissue Necrosis Factor – α (TNF-α), apoptosis pathways were stimulated in different shear situations; both pre-sheared and post-sheared application of TNF-α. Overall, this thesis will present a time course study on the varying expressions of DAPK and its role in apoptotic activation, in an effort to delineate roles of shear stress and DAPK in apoptosis pathways.

This thesis project aims to gain understanding of normal hemodynamic pathways for vascular function. The role of DAPK in mechano-transduction pathways of endothelial cells under applied shear stress was investigated. The role of shear stress on endothelial cells and their respective molecular cascades was examined in the context of DAPK. Fully understanding how shear stress effects the development of atherosclerosis would lead to identification of potential molecules involved in disease progression and treatment.

The questions and hypotheses that this thesis project will investigate are as follows:

- Does fluid shear stress directly modulate DAPK expression?
  - Hypothesis: Shear stress does affect DAPK expression.

- Does fluid shear stress suppress TNF-α induced apoptosis in endothelial cells, by influencing DAPK expression?
  - Hypothesis: Shear stress suppresses TNF-α induced apoptosis, in correlation to modulating DAPK expression.

2. SHEAR STRESS EXPERIMENTS

2.1 Fluid Flow Mechanics

For the shear stress experiments, a parallel plate flow chamber was used to simulate fluid shear stress on bovine aortic endothelial cells (BAEC). A parallel plate flow chamber is a rectangle-shaped chamber with multiple components. The flow chamber has a bottom section to house the glass slides containing the cells. There are gaskets to aid in sealing in between the sections. Also, the top section has inputs and outputs which the media flows through. There is a small gap height between the frame pieces to allow for fluid to flow across the cells. The controlled simulated shear was used to induce mechano-transduction signaling between the endothelial cells, mimicking the physiological hemodynamics.

To reproduce fluid flow through blood vessels, the flow chamber mechanics had to be developed for the flow shearing the cells. Blood flow within the cardiovascular system can be rather difficult to match, therefore some fluid mechanics simplifications had to be applied for the flow system. The Navier-Stokes equation, describing differential fluid flow movement for a relative system, was deduced from a possible three dimensional to a one dimensional flow system, only considering horizontal flow across an assumed infinite parallel plate [37]. This assumption is valid due to a small height to width ratio within our flow chamber.

$$\rho * \left(\frac{\partial u}{\partial t} + u\frac{\partial u}{\partial x} + v\frac{\partial u}{\partial y} + w\frac{\partial u}{\partial z}\right) = -\frac{\partial p}{\partial x} + \mu\left(\frac{\partial^2 u}{\partial x^2} + \frac{\partial^2 u}{\partial y^2} + \frac{\partial^2 u}{\partial z^2}\right) + \rho g_x \qquad \text{Eq. 2.1}$$

Equation 2.1 describes the 1-D Navier-Stokes equations used for our infinite parallel plate flow system.

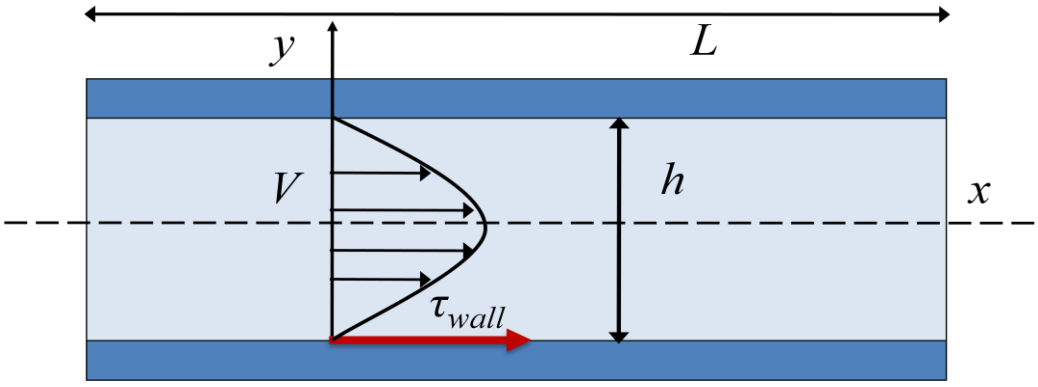

Figure 2.1 Fluid flow profile for the flow chamber

Additionally, the assumption of laminar flow is accepted based on low velocity flow, which in turn yields a low Reynolds number that describes the ratio between inertial forces and viscous forces of the flow. By neglecting the entrance length of the flow chamber, due to a smaller entrance length compared to the entrance length of the chamber, fully developed velocity profiles were accepted. Also presuming flow symmetry, fully developed parabolic flow was adopted as the flow occurring uniformly across the samples.

To further simplify the Navier-Stokes equation, steady state flow conditions were used to negate any time-dependant calculations for the flow system, assuming the flow would be stable within a short period of time after initial exposure of flow. Lastly, the flow was considered incompressible, due to very little to no pressure applied to the fluid within the system. Collectively, all of these simplifications helped to define a more approachable derivation of the Navier-Stokes equation, allowing for examination of the fluid movement and shear applied within the system.

When all of these assumption taken into consideration, one can reduce the 1-D Navier-Stokes equation down to a simplified representation of the fluid flow for the parallel plate flow chamber.

With assumptions of uniform flow in 1-D, fully developed parabolic, steady state, laminar, and incompressible flow, the Navier-Stokes equations becomes only dependent upon pressure and shear forces applied to the system as seen in Eq. 2.2.

$$0 = -\frac{\partial p}{\partial x} + \mu\left(\frac{\partial^2 u}{\partial y^2}\right) \qquad \text{Eq. 2.2}$$

Where p is the pressure, μ is the viscosity of the flow medium, and u is the x- direction velocity of the flow in the system.

To further evaluate the simplified equations, two specific boundary conditions are applied to define the flow within the chamber. Boundary condition 1 will imply a no slip condition at the wall-fluid interface, showing that the flow velocity will be zero at this interface. For the second condition, the flow is considered to be fully developed, implying that there is no change in the velocity at the center of the flow profile. At the center of the flow, the velocity is maximum, boundary condition 2.

$$y = 0, h \rightarrow u = 0 \qquad \text{[Boundary Condition 1]}$$

$$y = {}^{h}/_{2} \rightarrow \frac{du}{dy} = 0 \qquad \text{[Boundary Condition 2]}$$

Where h is the height of the flow chamber along the y-axis and the flow is along the x-axis.

Rewriting Eq. 2.2: $\frac{d^2u}{dy^2} = \frac{1}{\mu}\frac{dp}{dx}$

1st Integration: $\frac{du}{dy} = \frac{y}{\mu}\frac{dp}{dx} + C_1$ Eq. 2.3

2nd Integration: $u = \frac{y^2}{2\mu}\frac{dp}{dx} + yC_1 + C_2$ Eq. 2.4

Applying both boundary conditions: $C_1 = -\frac{h}{2\mu}\frac{dp}{dx}$; $C_2 = 0$

$$\frac{du}{dy} = \frac{y}{\mu}\frac{dp}{dx} - \frac{h}{2\mu}\frac{dp}{dx} \quad \rightarrow \quad \frac{du}{dy} = \frac{1}{\mu}\frac{dp}{dx}\left(y - \frac{h}{2}\right) \qquad \text{Eq. 2.5}$$

Definition of Shear Stress: $\tau = \mu\left(\frac{\partial u}{\partial y} + \frac{\partial v}{\partial x}\right)$; with $\frac{\partial v}{\partial x} = 0$ in $1 - D$. Eq. 2.6

Substituting Eq. 2.5: $\tau = \frac{dp}{dx}\left(y - \frac{h}{2}\right)$ Eq. 2.7

Volumetric Flow Rate $\rightarrow Q = \int_A \overline{V} * \overrightarrow{dA} = \int_0^h u * w\, dy = -\frac{1}{12}\frac{dp}{dx} * h^3$ Eq. 2.8

With $\overline{V}$ representing the average flow velocity integrated over the entire flow area, and w is the width of the flow chamber which is a constant value. In result, $\frac{dp}{dx}$ has to be less than 0 in order to have flow across the chamber. The average flow velocity is defined as the volumetric flow rate per unit depth, as seen in Equation 2.9.

Average Flow Velocity $\rightarrow \overline{V} = {}^{Q}/_{A} = \frac{\frac{-1}{12\mu}\frac{dp}{dx} * h^3}{h * w} = -\frac{1}{12\mu}\frac{dp}{dx} * h^2$ Eq. 2.9

Next, one must evaluate the maximum flow velocity, in order to develop a relationship to the average flow velocity.

After integrating: $\frac{du}{dy} = 0 = \frac{1}{\mu}\frac{dp}{dx}\left(y - \frac{h}{2}\right)$

u_max = $u\left(\frac{h}{2}\right) = \frac{1}{\mu}\frac{dp}{dx}\left(y^2 - \frac{yh}{2}\right)$; where $y = h/2$

$$u_{max} = -\frac{1}{8\mu}\frac{dp}{dx} * h^2 \qquad \text{Eq. 2.10}$$

After finding the average and maximum flow velocities, we can find a relation between the two, in order to manipulate the shear stress equation into variables that are known.

$$\frac{u\_max}{\bar{V}} = \frac{-\frac{1}{8\mu}\frac{dp}{dx}*h^2}{-\frac{1}{12\mu}\frac{dp}{dx}*h^2} = 3/2; \quad u\_max = \frac{3}{2}\bar{V} \qquad \text{Eq. 2.11}$$

Using the definition for the mass flow rate, $\dot{m} = \rho\bar{V}A$, Eq. 2.12, we can express the average velocity as: $\bar{V} = \frac{\dot{m}}{\rho A}$, Eq. 2.13. Next, we further simplify Equation 2.10 using our new variable relationships from Equation 2.13 to define the new pressure gradient relationship, as seen in Equation 2.14.

$$\frac{dp}{dx} = -\frac{8\mu}{h^2}u_{max} = -\frac{8\mu}{h^2}\left(\frac{3}{2}\bar{V}\right) = -\frac{8\mu}{h^2}\left(\frac{3}{2}\right)\left(\frac{\dot{m}}{\rho A}\right) \qquad \text{Eq. 2.14}$$

Now that the pressure gradient is defined, we can rewrite the shear stress equation that was previously defined in equation 2.7.

$$\tau = \frac{dp}{dx}\left(y - \frac{h}{2}\right) = -\frac{8\mu}{h^2}\left(\frac{3}{2}\right)\left(\frac{\dot{m}}{\rho A}\right)\left(y - \frac{h}{2}\right) = -\frac{12\mu\dot{m}}{h^2\rho A}\left(y - \frac{h}{2}\right) \qquad \text{Eq. 2.15}$$

Using the volumetric flow rate and mass flow rate, Equations 2.8 and 2.12, we already have defined $Q = \bar{V}A$ and $\bar{V} = \frac{\dot{m}}{\rho A}$. Therefore $Q = \frac{\dot{m}}{\rho}$; which can be inserted into the shear stress relationship.

When the shear stress equation is evaluated at y = 0, h; at the chamber walls, shear stress becomes:

$$\tau = -\frac{12\mu\dot{Q}}{h^2\rho}\left(y - \frac{h}{2}\right) \rightarrow \tau(0) = \frac{6\mu\dot{Q}}{hA} \text{ and } \tau(h) = -\frac{6\mu\dot{Q}}{hA} \qquad \text{Eq. 2.16}$$

Ultimately, the final form of the shear stress applied at the surface from the flow is dependent on the viscosity of the media, volumetric flow rate, height of the chamber, and the total flow area.

$$\tau = \frac{6\mu\dot{Q}}{hA} \qquad \text{Eq. 2.17}$$

Equation 2.17 displays all known variables to express the shear stress of the flow. This calculation will show what shear is applied to the cells, and just how we can vary the amount of shear applied by our system, specifically through varying the volumetric flow rate, Q.

2.2 Shear Stress Experimental Setup

For shear stress flow experiments, cells were grown on glass slides to approximately 100% confluency. In order to carry out the shear stress experiments, cells were placed in a flow chamber, attached to a flow loop placed in an environment chamber, to mimic physiological conditions. Figures 2.2 and 2.3 show the flow chamber setup that encloses the sheared cells.

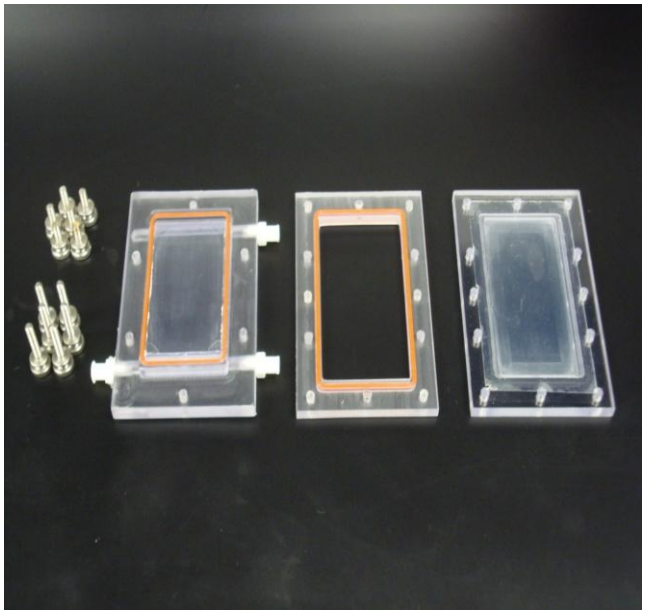

Figure 2.2 The three pieces of the cell flow chamber: top, middle, and bottom pieces.

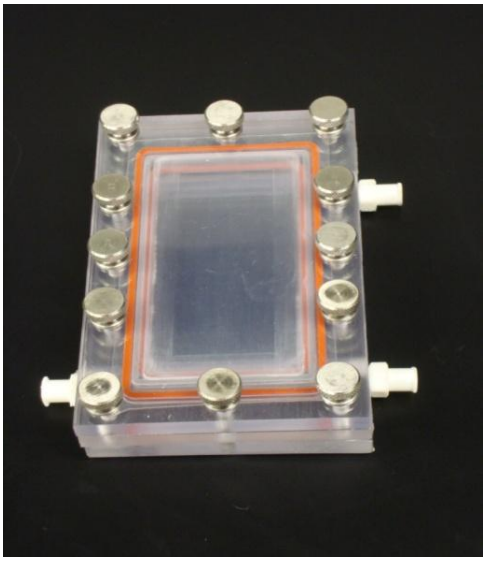

Figure 2.3 Combined flow chamber

The middle and bottom pieces of the chamber are held together by screws to house the glass slide containing cells. Media flowing into and out the top piece, through slits cut across, allowing for the flow to horizontally shear the cells. All three pieces are tightened together with screws and ready to be setup in the housing, shown above in Figure 2.3.

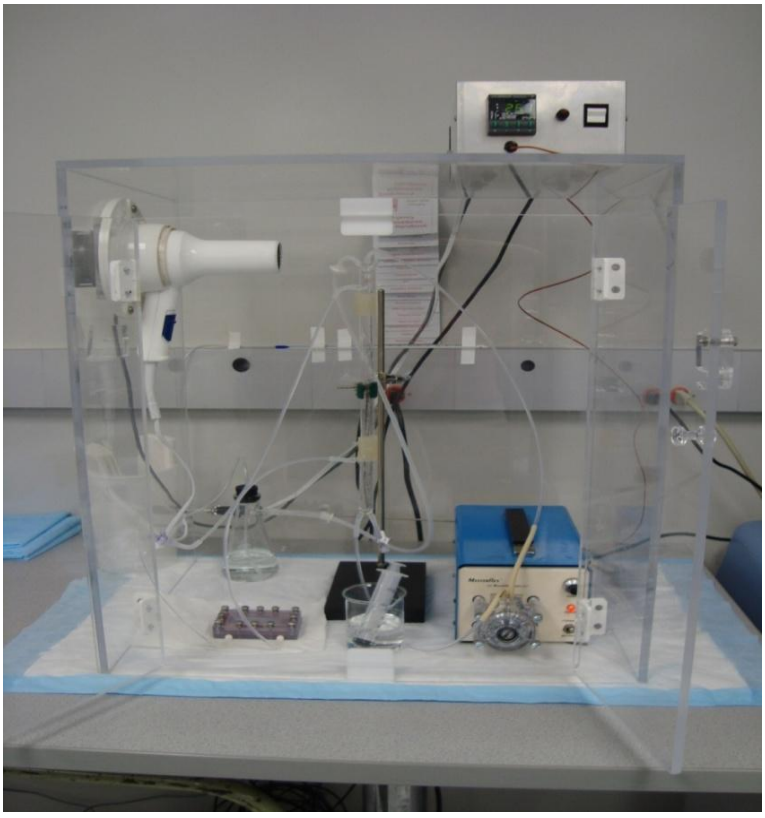

Figure 2.4 Housing environment for flow set-up with temperature control

In Figure 2.4, the housing environment contains multiple components in to run and regulate the flow experiments. On top of the plexiglass housing, there is a PSU and digital thermometer calibrated and set to keep the temperature inside the chamber at 37º C. There is a Masterflex rotating pump that cycles the flow media throughout the flow setup. Attached to the chamber, a modified hair dryer heats the chamber during experiments, controlled internally by a heat sensor probe and externally by the digital thermometer. When the temperature falls below the preset value, the hair dryer will turn on until the preset temperature has been restored for the housing environment.

The glass tube reservoir system consists of three different sections connected with silicone and Teflon tubing: a top section glass tube with three inlets and one outlet, a straight section glass tube, and a bottom section glass tube with one inlet and two outlets. For the top tube, there are inlets for CO_2, flow media, and an air release tube. The one

outlet is for distributing media leading to the flow chamber. As for the bottom section of tubing, there is an inlet that receives media flow from the attached flow chamber that returns to the bottom of the glass tube into the reservoir. The other inlet is plugged with a three-way stopper allowing for adding or subtracting media to the reservoir. From the reservoir, there is an outlet where the media is cycle back to the pump, eventually recycled to the top glass tube.

For running the shear experiment, the housing environment was brought to the temperature set at 37º C and 5% CO_2 air being pumped into the setup for cell viability and physiological pH control. The confluent cells attached to the glass slide are placed in the flow chamber setup. The flow chamber is hooked up to tubing and a peristaltic pump, which circulates media. After all the tubes are connected, 20mL of media is added to a three-way connector to fill the reservoir and to clear any air bubbles in the system. After all portions are filled with flow media, the clamp that was blocking flow to the inlet of the flow chamber can be removed. All air bubbles must be cleared from the flow chamber and any sections of the tubing to ensure constant shear flow to the cells, with steady state flow as one assumption used in deriving the flow mechanics.

Specifically, the shear stress is based on the constant fluid flow rate and the flow area of the system in the flow chamber. In order to change shear stress, the straight section of glass tubing could be varied changing the overall flow rate of the media, in turn changing the applied shear stress.

3. DAP-KINASE GENE EXPRESSION

3.1 DAPK and Shear Stress

The correlation between DAPK expression and specific shear flow profiles is thought to play a pivotal role in endothelial cell signal transduction processes. DAPK expression can further map its role in endothelial cell activities, when exposed to fluid flow. The DAPK protein expression was investigated using a time-course study comparing static cells (no shear) and cells exposed to various lengths of shearing.

In order to investigate the representative activation profiles, various molecular biology techniques were used to quantify protein and mRNA expression, under fluid shear stress. Understanding pre- and post-translational activity of DAPK can lead to an insight on the possible roles in shear-inducing signaling cascades, relative to specific endothelial cellular responses.

This section will address our first thesis question:

- Does fluid shear stress directly modulate DAPK expression?
    - Hypothesis: Shear stress does affect DAPK expression.

3.2 DAPK Protein Expression Analysis

3.2.1 Experimental Setup

For each of the shear stress experiments and analysis, all of the individual steps were mimicked using each of the following section descriptions. Cells are cultured and plated on glass slides. Next, cells are collected and analyzed depending on the specific molecule of interest, i.e. protein analysis or mRNA isolation. Subsequent steps are followed based on the specific mode of DAPK examination.

3.2.1.1 Cell Culture

Bovine aortic endothelial cells (BAEC; Lonza) were cultured using Dulbecco's Modified Eagle Medium (DMEM; SIGMA) with 10 % Calf Serum (NCS; SIGMA), 1 % L- glutamine (L-glut; SIGMA) and 2% Penicillin/Streptomycin (P/S; SIGMA). BAECs were cultured in tissue cultured flasks (T-75 flasks; Becton, Dickinson and Co.). The cell culture flasks contained 0.2 µm vented blue plug sealed caps, with 75cm^2 of cell culture area. The cells were stored in a 37°C incubator supplied with 5% CO_2. Cell media was changed for the cells on a regular basis, every day to every other day, to supply fresh nutrients and control the pH environment for the BAECs. The cell cultures were grown to 95% - 100% confluency, until the BAECs could be passed and collected to be plated for experimental shear runs. In order to collect cells, they were initially washed with Phosphate Buffered Saline (PBS; SIGMA) and subsequently incubated with Trypsin (SIGMA) for approximately 5 minutes at 37°C. Once the trypsin has detached the cell population, DMEM was added to deactivate the trypsin and to re-suspend the BAECs. The cell solution was collected in a 15mL tube and centrifuged at 2100 rpm for 5 minutes to pellet the cells. Once the pellet was collected, the cells were re-suspended in DMEM and plated on sterile glass slides for the shear stress experiments.

3.2.1.2 Protein Analysis

After shear experiments, the cells were lysed with RIPA buffer, in order to isolate and collect cellular protein, and scraped from the glass slide. The RIPA lysis buffer, containing 50mM sodium fluoride to maintain DAP-K phosphorylation, was combined with PMSF and a protease inhibitor (Sigma P-2714) to release cellular protein and to prevent protein degradation [38]. Once the solution was collected, the protein was isolated from cellular fragments leaving the respective sample to be further analyzed.

After collecting the samples, the concentration of protein for each sample was determined using a colorimetric protein assay. The assay displays protein concentrations based on specific absorbance values read using a spectrophotometer. In order to find the sample concentrations, an absorbance calibration curve was created using Bovine Serum Albumin (BSA) protein standard and specific dilutions with known concentrations. The protein concentration of each of the samples was calculated based on the calibration equation and where they fell relative to the known protein concentrations.

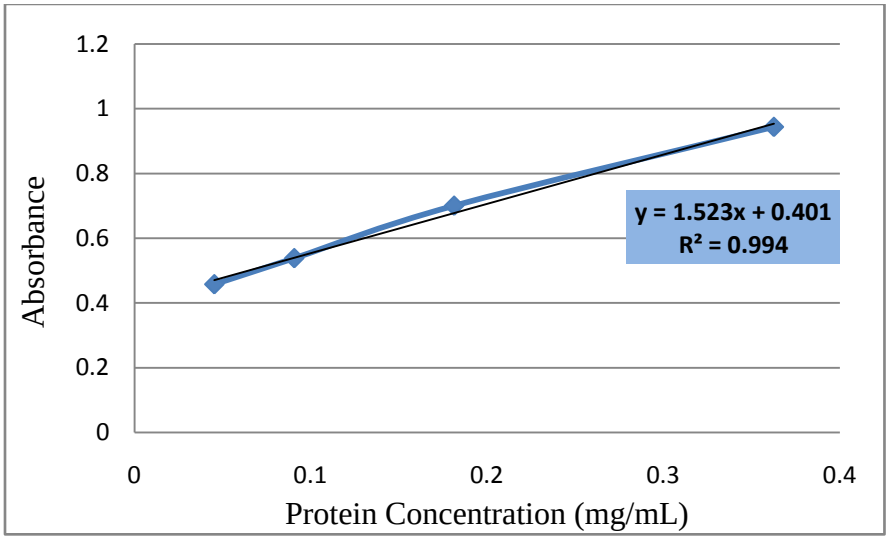

Figure 3.1 Sample protein calibration curve for protein concentration verification

3.2.1.3 Gel Electrophoresis

After calculating sample protein concentrations, DAPK protein values were investigated using Western immuno-blotting techniques. Using the protein concentrations, an equal amount of sample protein, protein dye, and sample buffer were loaded into the top of each well in a 10-well, pre-cast, poly-acrylamide gel. The loaded gel was run in MOPS running buffer at 180V for approximately an hour, or until the dye begins to run out of the bottom of the gel.

As the electrophoresis is run on the gel, the denatured proteins within each sample would run vertically down the gel, aligning based on the molecular weight (size) of each protein in the sample solutions.

3.2.1.4 Antibody Labeling

After running the gel through electrophoresis, the gel was placed on a nitrocellulose transfer membrane and run at 25V for 45 minutes to transfer the protein in the gel to the membrane surface. Next, the membrane was blocked in a blotto solution (5% non-fat milk powder in PBS + 1% Tween). The transfer membrane was blocked for 1 hour on a shaker at room temperature. After blocking, the membrane was then incubated in a primary DAPK antibody (DAPK55 antibody, overall DAPK protein, or DAPKPS308, phosphorylated DAPK) blotto solution at a 1:1000 dilution, approximately 5µL of antibody to 5mL of blotto. The membrane was placed on a shaker and allowed to incubate over night.

After the primary antibody incubation, the membrane was washed 3 times with PBS-T. Next, the protein membrane was incubated with a secondary antibody (Horse Radish Peroxidase, HRP) in blotto solution in a 1:5000 ratio dilution for 2 hours, approximately 1µL of antibody to 5mL of solution. After 3 washes with PBS-T, the membrane was put into a chemiluminescence reagent; contain equal parts of enhanced luminal and oxidizing agents [39].

The chemiluminescence reagent will fluorescently label the secondary HRP antibody that is conjugated to all primary DAPK antibody molecules that have attached to the DAPK proteins in each sample.

3.2.1.5 Molecular Imaging and Protein Quantification

Lastly, the membranes were imaged in a molecular imager (ChemiDoc XRS+; Bio-Rad Laboratories). The resulting images were used to quantify protein densities, using Bio-Rad Quantity One imaging software, for overall protein values in each sample. After DAPK protein images were analyzed, the labeling protocol was repeated with an Actin primary antibody, which was used as a protein loading control.

To quantify protein, blot images were analyzed using Quantity One 1-D analysis software. Western blots were imaged and uploaded into the analysis program. Next, rectangular boxes were placed on the each sample's targeted protein expression, such as overall DAPK, phosphorylated DAPK, and actin. Each protein box is drawn to the same sizes, and one box is drawn as a background to represent the color of the surrounding plot with no protein expression, subtracted as a baseline. Figure 3.2 is showing a Quantity One example of the protein quantification process, to demonstrate the analysis process after western blotting procedures.

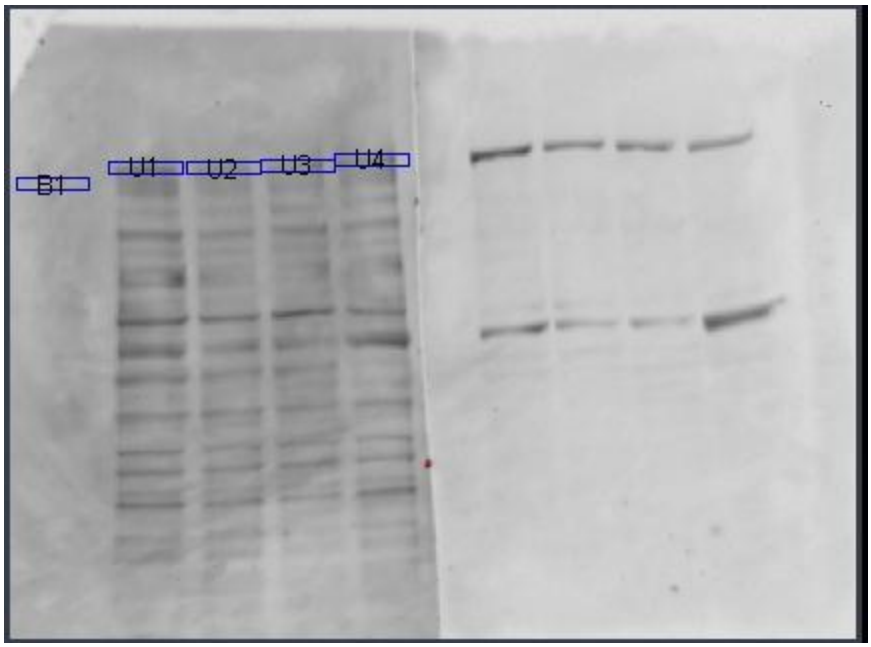

Figure 3.2 Sample Western blot image quantifying protein using Quantity One

After capturing the protein expression, a volume analysis is done to read the amount of target protein in each sample, minus the background read from box B1. Each sample is labeled with a different number and expressed in a volume analysis report, describing each of the volumes of protein expressed. See Table 3.1

Table 3.1 Volume analysis report from a sample DAPK protein analysis

Index	Name	Volume (INT*mm2)	Adj. Vol. (INT*mm2)	% Adj. Vol.	Mean Value(INT)
1	U1	318814.9533	**168013.2975**	31.85618766	13283.955
2	U2	260627.3472	**109825.6915**	20.82351747	10859.47167
3	U3	276170.6288	**125368.9731**	23.77060383	11507.10833
4	U4	275005.5087	**124203.853**	23.54969104	11458.56167
5	B1	150801.6557	**0**	0	6283.401667

Once the protein values were quantified for both DAPK and actin, a relative DAPK protein expression, with respect to actin, was recorded for each experimental sample.

3.2.2 Results

First, the influence of shear stress on DAP-K protein expression was investigated using various samples exposed to shear stress for varying amounts of time. Endothelial cells were plated on glass slides and grown to complete confluence. The different samples were in one of the four following time sheared categories: Static (no shear), 3 hr shear stress exposure, 6 hr shear stress exposure, and 8 hr shear stress exposure.

Static and sheared cells were analyzed in for overall and phosphorylated DAPK protein expressions, with results displayed in Figures 3.3 to 3.6. Proteins were collected from three different sets of experiments (n = 3), where cells from static, and 3, 6, and 8 hr of shearing conditions were lysed and collected. Western blot analysis was carried out on all samples, and images were quantified and analyzed as relative intensity compared to actin (loading control). Average relative intensities (DAPK/Actin) are presented in Figures 3.4 and 3.6. Representative Western blot image of the overall and phosphorylated DAPK are included in Figures 3.3 and 3.5.

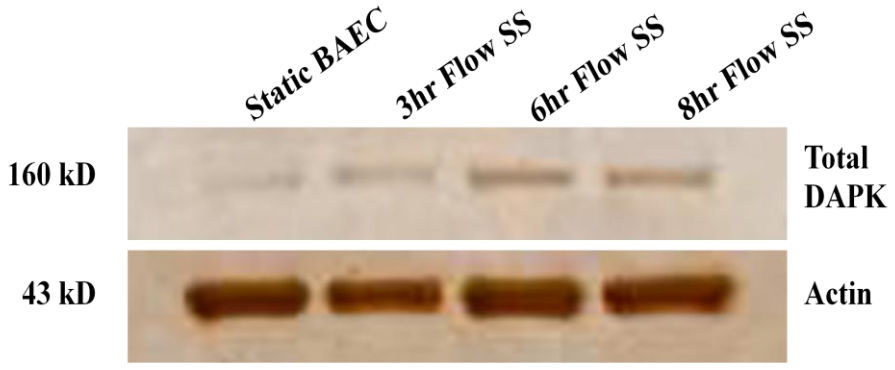

Figure 3.3 Western blots of overall DAPK expression over time (DAPK55)

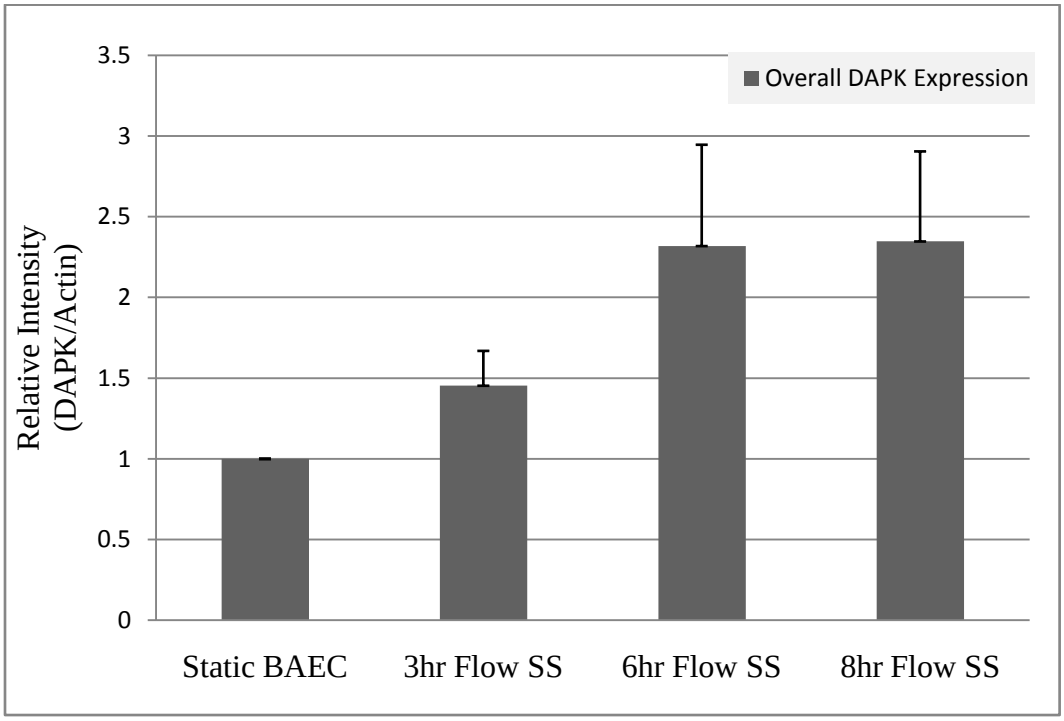

Figure 3.4 Overall DAPK protein expression – DAPK55

Figure 3.5 Western blots of phosphorylated DAPK expression over time (DAPK_P308)

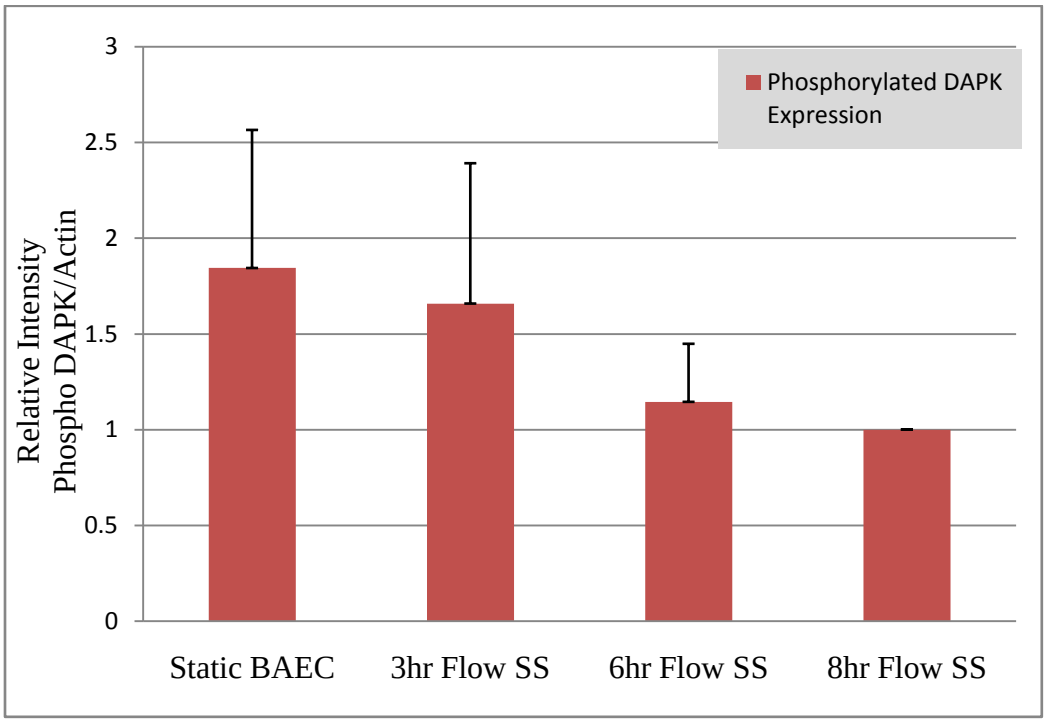

Figure 3.6 Phosphorylated DAPK protein expression – DAPK PS308

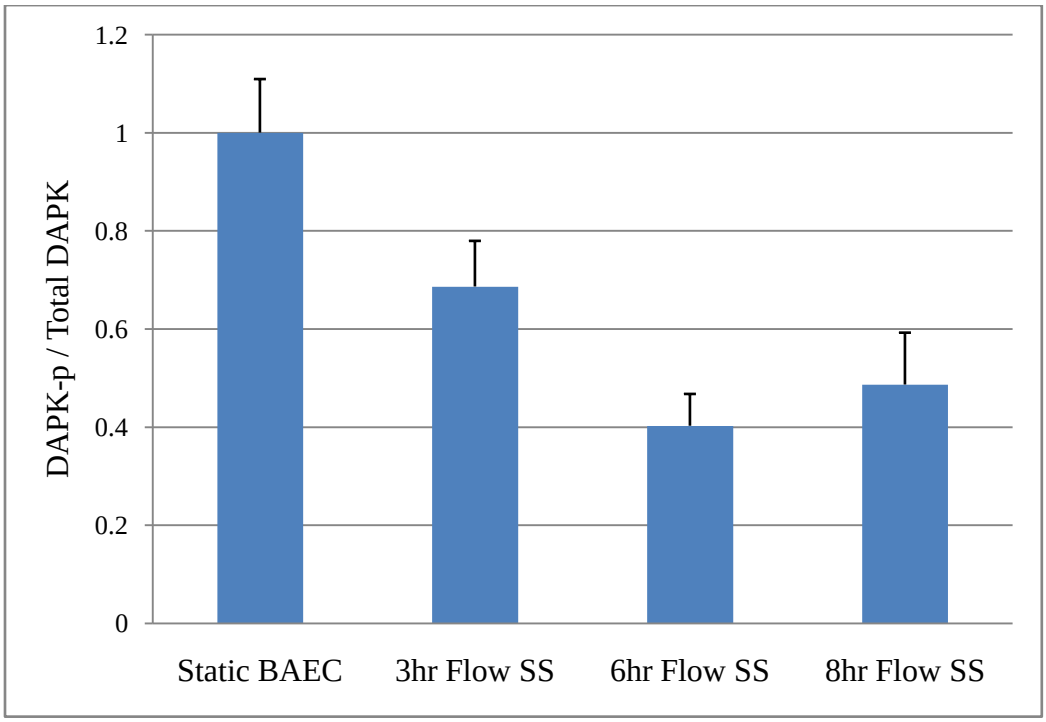

Figure 3.7 Phosphorylated DAPK expression with respect to total DAPK expression

Figure 3.7 shows the phosphorylated DAPK protein expression in terms of overall DAPK protein expression. In its basal state, DAPK is phosphorylated at Serine-308, and is activated through dephosphorylation. With the introduction of shear flow, DAPKPS308 becomes dephosphorylated, while overall all DAPK expression is increased. The data proposes shear stress decreases the concentration of DAPK-p, all the while increasing overall DAPK activity. With longer shear, the DAPK-p to DAPK ratio variation in protein expression could be attributed to the increase in DAPK protein being translated, which is originally in a phosphorylated state, increasing the ratio of DAPK-p to DAPK.

3.2.3 Discussion

As a whole, shear stress increases overall DAPK expression in endothelial cells, while a decrease in phosphorylation of DAPK was observed over time. We consistently observed a gradual increase in overall DAPK expression, as shown in Figures 3.2 and 3.3, with 6- and 8-hr sheared cells demonstrating a significant two-fold increase in DAPK expression, compared to static cells. The data suggests that expression of DAPK in time is at least in part modulated by elevated shear stress.

On the other hand, expression of phosphorylated DAPK seemed to decline initially after shearing (3 hr), but recovered after up to 8 hr. As cells are exposed to shear stress, DAPK phosphorylated at Serine 308 decreased initially. In other words, DAPK became more dephosphorylated. Since DAPK is dephosphorylated at Ser308 when activated, the data suggests that shear stress leads to dephosphorylation and activation of DAPK. After 8 hr, a slight increase in phospho-DAPK was observed, compared to 3 or 6 hr shear. Since DAPK in its basal state is phosphorylated, the increase in total DAPK production that we observed with extended shear may account for the increase in phospho-DAPK at 8 hr, and the more temporal pattern of phospho-DAPK under shear. Taken together, this data suggests shear stress increases DAPK expression in the long run, and activates DAPK by de-phosphorylation at Ser308 in the short term.

3.3 DAPK mRNA Expression Analysis

3.3.1 Experimental Setup

After outlining the DAPK protein expression profile, the pre-translational DAPK activation was explored, to further define the roles of shear in the DAPK signaling cascade. Just as with the DAPK protein experiments, Bovine aortic endothelial cells were plated and sheared at varying time points, to lay out the DAPK mRNA expression profile. mRNA expression was examined using real time RT-PCR, which further explains the temporal activation of DAPK with shear stress in endothelial cells. The mRNA expression profile was expected to confirm the DAPK protein results and the corresponding pattern of gene expression due to applied shear. For the mRNA experiments, both the shear stress experimental setup and cell culture procedures are the same as previously described in Sections 2.2 and 3.2 respectively

3.3.1.1 RNA Isolation

After each respective shearing experiment, cells were collected to isolate purified total RNA, and successfully removing genomic DNA. In order to carry out the process, Qiagen's RNeasy Plus Mini Kit was used in a sterile, RNase-free environment [40].

To start, cells were trypsinized to detach and collect them from the glass slides. From there, cells were disrupted by adding approximately 350 µL of Buffer RLT Plus, which contains β-mercapto-ethanol. Cells were homogenized by pipetting and transferred to a gDNA eliminator spin column. The spin column was placed in a 2 mL collection tube and centrifuged at 10, 000 rpm for 30 seconds, in order to separate the genomic DNA from the solution. Next, 350 µL of molecular biology grade 70% ethanol was mixed with the flow through solution collected from the spin column.

The solution was next pipetted into an RNeasy spin column, which contained a 2mL flow collection tube. The lysate was centrifuged in the RNeasy spin column at 10, 000 rpm for 15 seconds. Then, 700 µL of Buffer RW1 was added to the RNeasy spin column and spun at10, 000 rpm for 15 seconds. After centrifugation, the next two steps involve adding 500µL of Buffer RPE to the spin column, which is again spun at 10, 000 rpm. The first addition of Buffer RPE initially calls for 15 seconds centrifugation. After adding another 500µL of Buffer RPE, the column is spun for 2 minutes, effectively drying the spin column of any leftover ethanol. Lastly, 55 µL of RNase-free water is added to the RNeasy spin column and centrifuged for 1 minute, which will elute the purified RNA. After isolating the RNA, each sample was stored in RNase-free water at 20º C, prior to performing any reverse transcription procedures.

Table 3.2 RNA isolation protocol

Step	**Action**	**Solution**	**Volume (µL)**	**Spin @ 10,000 rpm**
1	trypsinize			
2	homogenize	RLT (lysis buffer)	350	
		transfer to		
3	gDNA eliminator			2 min.
4	Add to Flow Through	70% ethanol		
		transfer to		
5	RNeasy spin Column			15 sec.
6	Add/Spin	Buffer RW1	700	15 sec.
7	Add/Spin	Buffer RPE	500	15 sec.
8	Add/Spin	Buffer RPE	500	2 min. (dry)
9	Elute RNA	water	55	1 min. (collection)

3.3.1.2 Reverse Transcription

Following RNA isolation, the next step was to perform reverse transcription on the RNA molecules, in order to create cDNA of the RNA expressed by each sample. The RNA goes through reverse transcription to become a copy of DNA that transcribes that specific RNA molecule. The RNA has to be reversed into cDNA to subsequently quantify overall mRNA expression, using a real-time polymerase chain reaction protocol.

Using the High Capacity cDNA Reverse Transcription Kit (Applied Biosystems), the single-stranded collection of sample RNA was converted in to cDNA [41]. Initially, 10x RT buffer was added to RNase-free water in the sample tube, to help present the optimal physiological conditions for the reverse transcription to occur. Additionally, 10x random primers were added to the solution in order to present templates for transcription back into cDNA. To generate the cDNA, Deoxynucleoside triphosphates (dNTP) were added to the mix solution, aiding the primers in the conversion process. MultiScribe™ MuLV reverse transcriptase, the enzyme that catalyzes the conversion of RNA into cDNA, is added to the mix before adding the sample RNA solution to be transformed back into DNA.

After adding specific quantities of each reverse transcription component, each respective sample solution was placed in a thermal cycler. Initially, the samples are incubated at 25ºC for 10 minutes, before being ramped up to 37 ºC for 2 hours. After synthesizing cDNA from the thermal cycling, the samples are then held at 4 ºC to stop synthesis and preserve the cDNA sample.

Now, the sample can be further processed using real-time PCR to amplify target DNA and quantify overall mRNA expression results. Table 3.3 gives a reverse transcription protocol for one tube of sample RNA, and the cycling procedure used for the samples.

Table 3.3 Reverse transcription sample protocol (per sample)

Solution	1 tube
Water	9.2 µL
10x RT Buffer	2 µL
10x Random Primer	2µL
25x dNTP's	0.8 µL
MultiScribe™ Reverse Transcriptase	1 µL
Sample RNA	5 µL

Thermal cycler	
Temp.	**Time**
25°C	10 minutes
37°C	2 hours
4°C	Hold

3.3.1.3 Primer Development

After reverse transcription, the resulting cDNA sample could be cycled using polymerase chain reaction mechanisms (PCR). PCR is used to amplify small amounts of DNA, by several orders of magnitude, to be able to quantify overall target DNA amounts, compared to the expression of a reference gene.

Before PCR sampling, a specific primer template for DAPK and GAPDH, reference gene, had to be developed for DNA amplification. Primers, short DNA strands, are composed of specific complementary sequences for the target gene. The primers are very specific sequences to replicate only that certain target gene [42].

As PCR cycles temperatures, the primer DNA is used as the template, binding to target DNA and replicating several times over, exponentially increasing the amount of target DNA. Figure 3.8 shows the primer binding procedure.

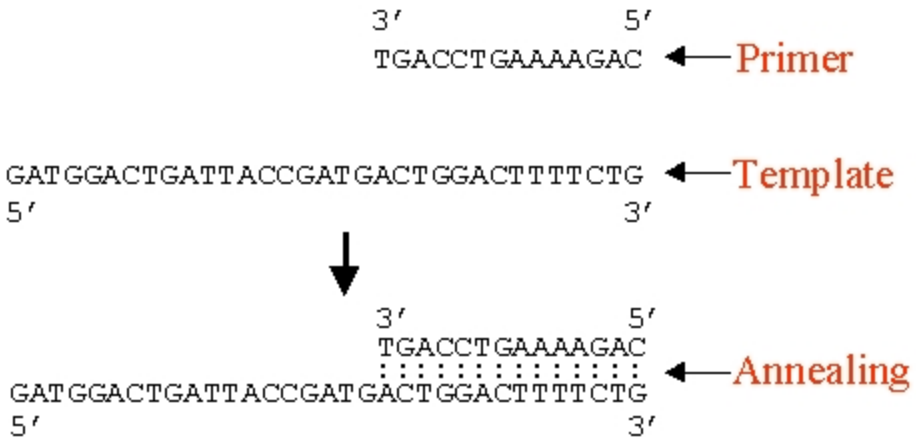

Figure 3.8 Complementary primers binding to template DNA [43]

To create highly specific primers, NCBI Primer-BLAST tools [44] were used to choose potential primer pairs based on mRNA sequences of bovine DAPK and GAPDH (reference gene). The actual mRNA sequence for each target gene expression were input into the Primer-BLAST program, specifying bovine and product lengths less than 150 base pairs.

Primer pairs had to have a product length of 150 or less for optimal real-time PCR results. Once potential primer pairs were found for each gene, the primer pairs were then input into the NCBI Nucleotide BLAST program make sure the primers were highly specific to each target gene, and no other genes would be amplified by mistake.

From the possible primer selections, a successful primer pair for each gene was identified to use for real-time PCR expression. Primers are presented in Table 3.4 on the following page:

Table 3.4 DAPK primers used for real time RT-PCR experiments

Gene	Forward Primer	Reverse Primer
DAPK	5'-CAAGCCGGCAGTGTCCGTGA-3'	5'-CAGTGCGGATGGTGGGACGG-3'
GAPDH	5'-CATTGACCTTCACTACATGGT-3'	5'-ACCCTTCAAGTGAGCCCCAG-3'

In Table 3.4, both a forward and reverse primer is presented for each of the respective genes. Both primer strands are needed due to the sequence reading activity of the enzymes, and the way the DNA is setup in an anti-parallel arrangement. Both primers anneal to the target DNA, extending one direction from the 5' to 3' end (forward) and extending in the opposite direction from 3' to 5' (reverse).

3.3.1.4 Real Time RT-PCR

As previously mentioned, real-time polymerase chain reaction is a process that exponentially amplifies small amounts of target DNA, while detecting the fluorescence of the sample quantifying specific gene expression quantities as PCR is cycled. To run the PCR experiment, the Applied Biosystems 7500 Fast Real-Time PCR System was used for each of the samplings.

First, SYBR Green PCR Master mix (Applied Biosystems) was combined with RNase-free water, in each tube depending on the number of desired PCR reactions. Next, each target gene's forward and reverse primers (DAPK or GAPDH), as shown in Table 3.4. Lastly, each cDNA template was added to their own PCR tube, mixed with one reaction aliquot of the SYBR-Primer solution. Table 3.5 displays the specific distribution of each of the solution components, per reaction.

Table 3.5 Real time RT-PCR solution protocol (per reaction)

Solution	Amount
Water	5.6 µL
SYBR Green	10 µL
Forward Primer (10 µM)	1.2 µL
Reverse Primer (10 µM)	1.2 µL
cDNA template	2 µL

Once each reaction solution is mixed, the samples are placed in the Real-Time PCR System to begin amplifying the target DNA. Using the software, all of the specific parameters for the relative quantification (ddCT) plate study were input, along with the cycling times and temperatures for each amplification step, as shown in Table 3.6. As the temperature is cycled, the cDNA is denatured at 95°C allowing for the temperature stable polymerase to extend new DNA from the primers. Next, the temperature is cooled to 60°C to allow for the primers to bind the template DNA. Subsequently, the temperature is ramped back up to 95°C for the polymerase to amplify template DNA, all while fluorescently labeling target DNA with SYBR green for real time quantification of gene expression [45].

Table 3.6 Thermal cycler for the real time PCR process

Thermal Cycler Profile			
Stage	**Repetitions**	**Temperature**	**Time Held**
1	1	50.0 °C	2:00 minutes
2	1	95.0 °C	10:00 minutes
3	40	95.0 °C	0:15 seconds
		60.0 °C	1:00 minute

3.3.1.5 Statistical Analysis

In order to verify the statistical significance of the results, the standard error of each subset was calculated. Additionally, each sample set was compared to the baseline sample set to make sure that there is statistical difference in the subsets and verifies the plots shown. Using a standard t-test comparing two sample sets, a probability of likelihood (p-value) that the sample sets were the same was determined. The p-value is a probability of obtaining a result as extreme as the one observed in the samples. With the lower the p-value, this represents the less likely the result of a similar occurrence, and consequently the more statistically significant the observed results become, usually with a p-value less than 0.05 to 0.01 being sufficient for verification.

3.3.2 Results

3.3.2.1 mRNA Expression Results

Once the PCR amplifications are complete, the results of the real time quantification were analyzed. The SYBR green fluorescence expressed by the new DNA was monitored over the progression of PCR cycling. A plot of the fluorescence intensity at each PCR cycle is developed. A user-defined fluorescence threshold for the samples is set, where there is detectable differences in samples being compared. The threshold cycle (C_T value) is defined as the PCR cycle number at which that respective sample has crossed the fluorescence threshold.

Figure 3.9 is a typical plot of showing the fluorescence intensities plotted against the PCR cycle number. Once a threshold is set at a difference in expression, the cycle thresholds can be recorded. From these C_T values, a representative fold expression increase is calculated between the compared samples.

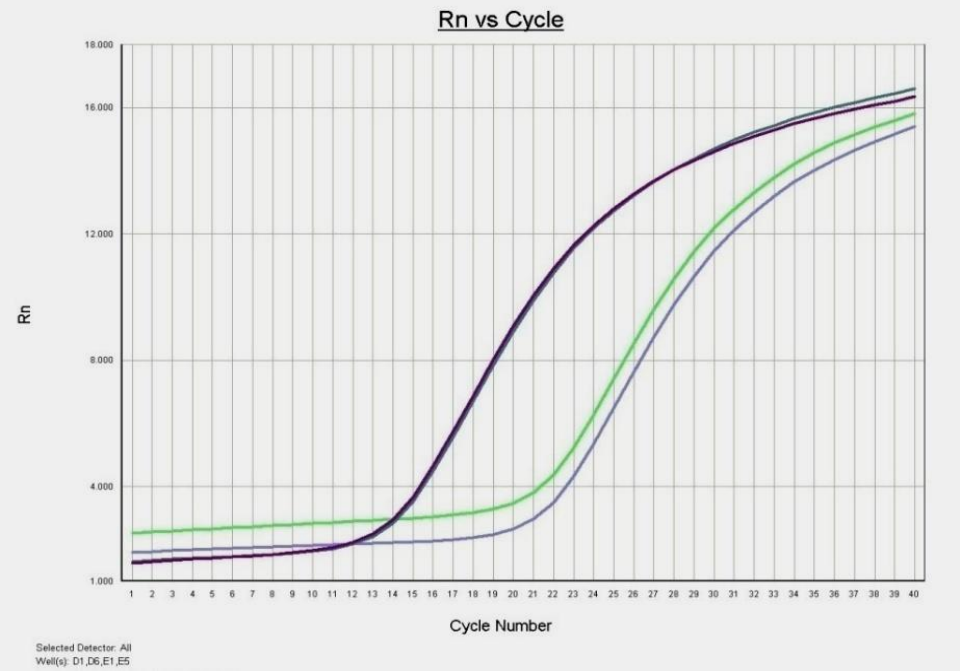

Figure 3.9 RT-PCR amplification plot between static and 8hr shear stress

To calculate the fold increase in DAPK mRNA expression, the $2^{\Delta\Delta Ct}$ method was used [46]. The ΔC_t of the control and experimental samples was calculated from the threshold cycle of the target gene minus the threshold cycle of the reference gene (GAPDH).

3.3.2.2 Fold Increase in DAPK Gene Expression

Both gene amplification efficiencies were assumed to be approximately 100%. This assumes that with each PCR cycle, one DNA molecule will be increased to two DNA molecules. Using this assumption, the fold increase of each sample was calculated, after PCR cycles, using the below equation:

$$(2)^{\mathbf{DAPK\_\Delta Ct - GAPDH\_\Delta Ct}} = 2^{\mathbf{\Delta\Delta Ct}} \text{ fold increase in DAPK} \qquad \text{Eq. 3.1}$$

To begin with, mRNA from cells under either static or 8 hr shear condition was isolated, followed by reverse transcription to cDNA. Figure 3.9 is an amplification plot from the first DAPK real-time RT-PCR experiment. Our data shows that there was a 1.09 fold increase in 8hr SS mRNA compared to static cells. The small fold-increase in mRNA, when compared with the protein intensity plot (Figure 3.4), does not correlate to the overall increase in DAPK protein at 8 hr shear.

It was assumed that the mRNA increase occurred much earlier after shear, resulting in the ultimate DAPK protein increase at 8 hr. Data from shorter shear stress experiments were needed to determine mRNA expression changes due to shear stress, to correlate with the overall DAPK protein expression over time. From Figure 3.10, the small difference in gene expression is shown by the respective average PCR cycle threshold for the samples.

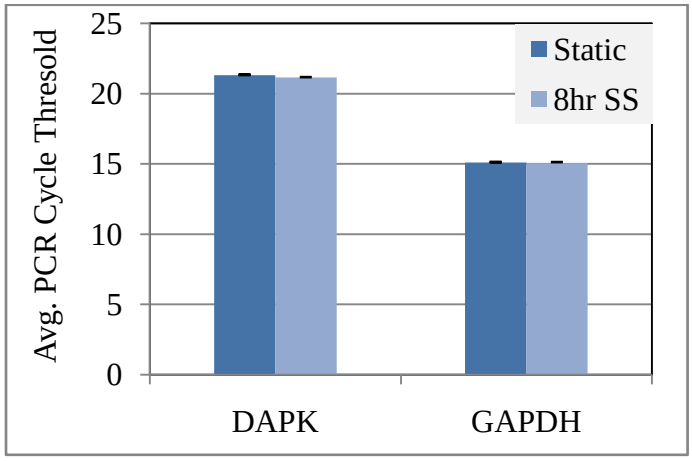

Figure 3.10 Average cycle threshold values for static and 8hr SS samples

To further evaluate the time course expression of DAPK, shear stress experiments were conducted at various lengths of time intermittently between no shear and 8 hours of applied shear. After each shear experiment, these cells were followed through same RNA isolation, reverse transcription, and RT-PCR protocols, as previously described.

Eventually, each of the cell samples' RT-PCR results lead to relative cycle threshold values. These results were used to calculate the DAPK mRNA fold increase at each shear time point compared to the static (no shear) DAPK mRNA expression. In Figure 3.10, the average fold increases of each sample were plotted according to the amount of time sheared. Each of the shear experiments were repeated at least three different times, in order to obtain an accurate representation of the DAPK mRNA expression profile.

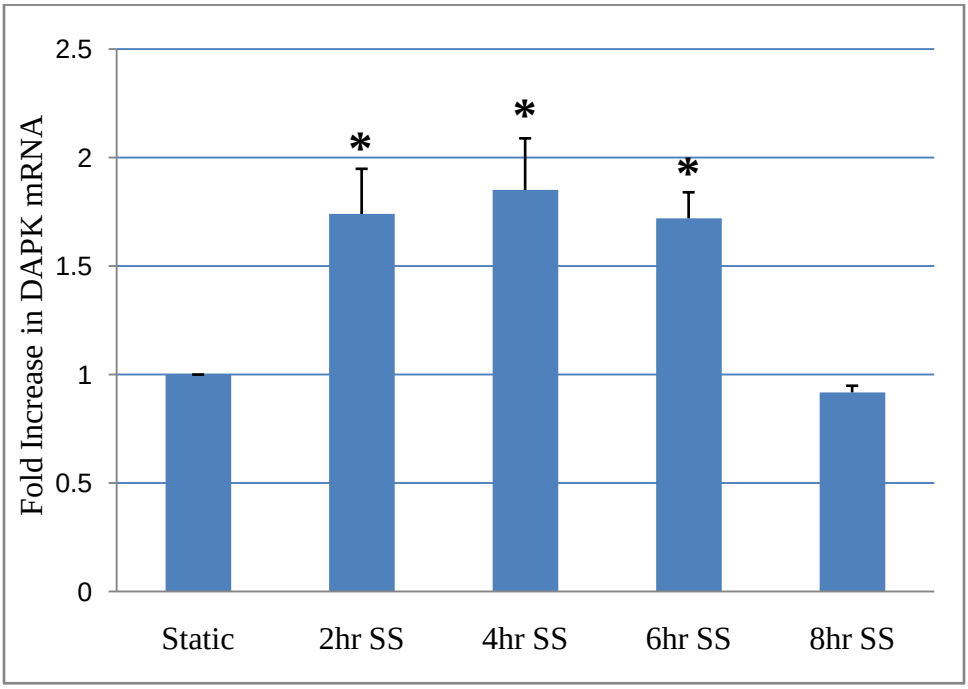

Figure 3.11 Fold increases of DAPK mRNA expression over varying time sheared, with * $p < 0.01$

3.3.3 Discussion

Overall, the DAPK mRNA expression profile was experimentally developed in a similar manner to the protein expression analysis. In comparison, the DAPK mRNA transcription increase precedes DAPK protein translation increase, relative to the time that the BAECs were sheared. The DAPK mRNA expression shows a temporal regulation pattern, as initially, the mRNA is up-regulated due to applied shear. After 4

hours of applied shear, the DAPK mRNA expression peaks at about twice the basal level of mRNA expression. Yet, as the shear continues, the mRNA expression begins to recede toward the basal level, to eventually display a small down-regulation at 8 hours of shear.

In relation to DAPK protein expression, the initial up-regulation of mRNA closely follows what was shown with the overall increase in protein across 8 hours of shear stress. On the other hand, the mRNA expression decrease in greater than 4-6 hours of shear was not seen in the overall DAPK protein expression. Longer exposure to shear stress might give an insight on the trajectory of overall DAPK protein expression, as well as other possible long term cellular responsibilities. Similarly, the extended shear will help gain an understanding on if the mRNA expression recovers in response to these longer periods of shear stress, and just how the endothelial cells respond in the long run.

Taken all together, the DAPK mRNA is initially elevated due to fluid shear stress exposure. Yet with continued shear, DAPK mRNA shows a decrease in levels of transcription. The transient mRNA activation coincides with a protein expression increase in overall DAPK. The data suggests that shear stress regulates DAPK expression, and that DAPK potentially plays a role in endothelial cellular mechano-transduction processes, as seen in its overall gene expression profile.

4. SHEAR STRESS AND APOPTOSIS

4.1 The Role of Shear in Apoptosis

Apoptosis, programmed cell death, is a highly-regulated cellular process required to maintain tissue homeostasis. This process is activated in various ways through stimuli and signal communication cascades. When apoptosis is signaled, the cell begins chromatin condensation and cell shrinkage in the early stage. Next, the nucleus and cytoplasm fragment, forming membrane-bound apoptotic bodies that are subsequently consumed by phagocytes. In contrast, cells can also undergo a separate form of cell death, necrosis, which is a where cells lose homeostasis, swell, and breakdown due to physical or chemical trauma. Consequently, the release of intracellular components can damage to surrounding cells or tissue, often causing immune response and inflammation [47].

Apoptosis is an important process during normal cell turnover processes and in aging. Yet, deregulation of apoptotic cascades has also been linked to various diseases, such as cancer, atherosclerosis, Alzheimer's disease, and Parkinson's disease. Due to its important role in cell processes and possibility of cell dysfunction, apoptosis and its connected signaling procedures, such as signal transduction, are extensively researched cellular processes.

Apoptosis can be detected using various methods, such as TUNEL (TdT-mediated dUTP Nick-End Labeling), Annexin-V staining analysis, measuring alterations in cell membranes, In situ end labeling, DNA laddering for the detection of DNA fragmentation in cell samples, as well as the quantification of apoptosis-related proteins, such p53

protein. Specifically, the thesis objective was to study the effects of applied shear stress on aortic endothelial cells, which line artery walls, and the resulting changes in cellular apoptosis. Shear due to flow can cause apoptosis signaling activation or inhibition for cells, depending on both environmental and local flow conditions. Certain cytokines can illicit apoptosis activation, such as in IL-1β or TNF-α addition.

On the other hand, in the presence of cytokine activation, fluid shear stress has been shown to inhibit certain apoptosis cascades and decrease overall cell turnover [47]. Therefore, As a result, the research goal was to investigate shear stress influence on apoptosis, in an effort to correlate previously examined DAPK expression patterns. All experimental samples and shear stress runs were repeated at least three times, using each research method, for statistically relevant verification of overall apoptosis results. Additionally, p-values for each experiment were calculated to verify statistical significance of the various sample sets.

This section will address the second thesis question:

- Does fluid shear stress suppress TNF-α induced apoptosis in endothelial cells, by influencing DAPK expression?
    - Hypothesis: shear stress suppresses TNF-α induced apoptosis, in correlation to modulating DAPK expression.

4.2 Experimental Setup

For apoptosis research, two of the more widely used techniques were utilized for the cell samples: flow cytometry and fluorescence microscopy. Fluorescence-activated cell sorting (FACS) allows for quantitative fluorescence analysis using flow cytometry.

FACS, a specific type of flow cytometry, is a technology that runs cell suspensions through a light-scattering machine that categorizes cell events based on the fluorescence given off by the individual cell.

As the cells are passed through beams of light one at a time, scattered and fluorescent light is collected by the detectors analyzing each cell's light characteristics.

As for fluorescence microscopy, cells are fixed and imaged on the individual glass slide. The cell slides are then fluorescently marked using specific fluorophores to label desired cellular components. After the samples are labeled, the slides can be imaged using a fluorescence microscope, which passes excitatory light through its objective. This excitatory light passes through sample and excites the fluorophore-labeled cellular components. Images can be taken of the cell samples for further analysis and/or quantification of certain targets.

To examine DAPK activity under apoptotic conditions in endothelial cells, we incubated BAEC with TNF-α for up to 48 hrs and lysed cells for protein samples at 6, 24, and 48 hours.

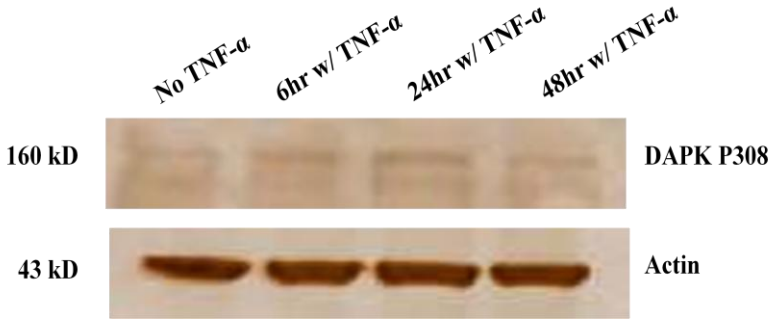

Figure 4.1 TNF-α activation of DAPK P308

Following Western blot analysis, it was observed that while overall DAPK expression remained the same (data not shown), phospho-Ser308 DAPK also demonstrated a temporal response to TNF-α (Figure 4.1).

At 48 hr treatment with TNF-α, the most significant decrease had occurred in phospho-DAPK, or the most significant increase in dephosphorylation or activation of DAPK. And at 24 hr TNF-α treatment, we observed the greatest increase in phospho-DAPK. The western blot data suggests a dynamic DAPK phosphorylation process with TNF-α treatment.

4.2.1 Annexin V/PI - Flow Cytometry

Apoptosis was analyzed using the FITC-Annexin V (BD Pharmingen) based staining of endothelial cells treated with TNF-α, under either static or shearing conditions (SS). Annexin V, a phospholipids binding protein, attaches to the membrane phospholipid, phosphatidylserine (PS). Specifically, PS becomes exposed to the outer cellular membrane in the early stages of apoptosis. Therefore, Annexin V, conjugated with Fluorescein (FITC), can bind the exposed phospholipids and cells can be analyzed using FACS cell sorting. In addition to Annexin V, cells can be co-stained with propidium iodide (PI), exclusively permeable to dead cells, to distinguish between apoptotic cells and necrotic cells within the cell samples [48].

To begin with, three different cell samples were grown for apoptosis analysis: Control (no shear or TNF-α), Static + TNF-α, and 6hr Sheared + TNF-α. With the addition of TNF-α, apoptosis was activated pre-shearing to see the possible protective role of applied shear, as well as possible long-term anti-apoptotic signaling of cellular constructs. TNF-α (Sigma) was added to the cell media at 10 ng/mL, in order to elevate apoptotic activity. In order to maximize the activation of the apoptotic cascade, cells were incubated with TNF-α for 18 – 20 hrs overnight.

The sheared sample was run in a shear stress experiment with the running media also containing 10 ng/mL of TNF-α, so both samples could continue incubation with the apoptosis activator. After experiments, cells were detached gently using non-enzymatic Cell Stripper (Cellgro Mediatech), collected, and stained with PI and FITC for Annexin

V. Annexin V stained apoptotic cells, while Propidium Iodide stained necrotic cells. For analysis, the FACScan flow cytometer (BD Biosciences) categorized the cell sample's fluorescent characteristics, in addition to quadrant quantification by the CellQuest software [49].

4.2.2 TUNEL Staining - Fluorescence Microscopy

For fluorescence microscopy analysis, apoptosis was identified using TUNEL staining DNA labeling. The TUNEL (TdT-mediated dUTP Nick End Labeling) assay uses nuclear DNA degradation, as seen in apoptotic process, to label the cells undergoing apoptosis. During apoptosis, nuclear DNA begins to degrade and exposes large amounts of 3´-hydroxyl ends. Terminal deoxynucleotidyl transferase (TdT) adds deoxynucleotide triphosphates to the exposed hydroxyl groups of the degraded DNA. Along with the TdT, there is a conjugated fluorescent molecule to label these DNA nick sites, which can be used to quantify the number of cells undergoing apoptosis within a cell sample [50].

Cells samples were grown on glass slides to confluency, as apoptosis was activated both pre- and post-shearing. The experimental samples were conducted as follows: control BAEC, static + TNF-α, 6hr sheared + TNF-α, and 1hr pre-shearing followed by the addition of TNF-α. After finishing shearing experiments, cells were fixed with 4% parafomaldehyde and permeabilized with 0.2% Triton X-100, before being stained with for apoptosis analysis.

For TUNEL staining, sample slides were incubated with terminal deoxynucleotidyl transferase enzyme and nucleotide-Fluorescein (green fluorescence) label solution for 1-2 hours (In Situ Cell Death Detection Kit, Fluorescein). Following TUNEL staining, cells were labeled for nucleus by using Hoechst Blue solution at a 1:1000 dilution in PBS solution (blue fluorescence).

After sample labeling, cell slides were imaged using Leica DMI600 B inverted fluorescence microscope system, for both cell phase and fluorescence images. Leica Application Suite program was used for image acquisition. Image analysis was done using Image Pro Analyzer 6.2 software, to count the number of TUNEL positive cells, as well as total cell nucleus counts per image.

For each sample cell slide, cell phase, green fluorescence protein (GFP), and DAPI nuclear images (Fluorescence for Hoechst Blue), (10 – 12 of each type) were acquired, at various locations throughout the slide. All three types of images (phase, GFP, and nucleus) were taken at each location before moving to a different area on the slide.

Once all the samples were imaged and analyzed, the average percent of apoptotic cells per population was calculated based on the number of TUNEL positive cells, out of the number of total cells (nucleus counts) per image. From the final results, overall apoptosis activation of the different samples were compared between control, static + TNF-α, sheared + TNF-α, and pre-shearing conditions.

4.2.3 TUNEL Staining – Flow Cytometry

To verify the fluorescence microscopy results, the TUNEL staining experimentation was repeated using flow cytometry. The identical four cell samples were investigated as previously described: control, static + TNF-α, sheared + TNF-α, and pre-sheared cells.

After finishing shearing experiments, cells were detached gently using non-enzymatic Cell Stripper (Cellgro Mediatech) and collected. Cell suspensions were fixed with 1% parafomaldehyde and permeabilized with 0.2% Triton X-100, before being incubated with TUNEL staining for apoptosis analysis.

For analysis, the FACScan flow cytometer (BD Biosciences) analyzed each cell suspension's fluorescent characteristics. For each flow cytometry run, the populations of TUNEL positive cells were quantified using the CellQuest software [49].

4.3 Results

4.3.1 Annexin V/PI - Flow Cytometry

In the early stages of investigating apoptosis, the first analysis technique involved staining cells with Annexin V and Propidium Iodide, followed by flow cytometry cell analysis. In order to set up the classification quadrants for flow cytometry, specific controls had to be analyzed before the sample analysis.

In Figure 4.2, all three controls are displayed. A represents cells with no stain; B has cells stained with Annexin only, representing viable and apoptotic populations; and C is cells stained with Propidium Iodide only, representing viable and necrotic (dead) cell populations.

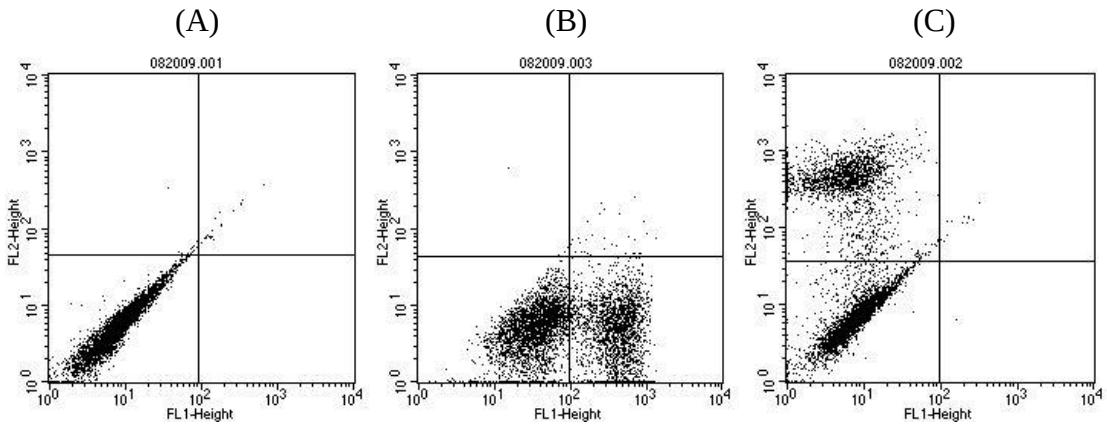

Figure 4.2 (A) No stain BAEC control; (B)Annexin V only (apoptosis) control; (C)Propidium iodide only (necrotic) control

From the three controls, the quadrants were adjusted based on the response in all three flow cytometry scenarios: Lower left: viable; lower right: apoptotic; upper left: necrotic; upper right: late stage apoptotic/necrotic.

After defining the cell quadrants, the samples stained with both Annexin V and PI were analyzed with the flow cytometer. The three cell samples were run until 10,000 cell events were accumulated. Once all samples were finished, the number of events in each quadrant were identified and recorded. Those cells categorized with both stain components were categorized as late stage apoptotic/necrotic cells.

In Figures 4.3 – 4.5, the one of the three flow cytometry results are presented for static BAEC, static + TNF-α, and 6hr sheared + TNF-α cell samples.

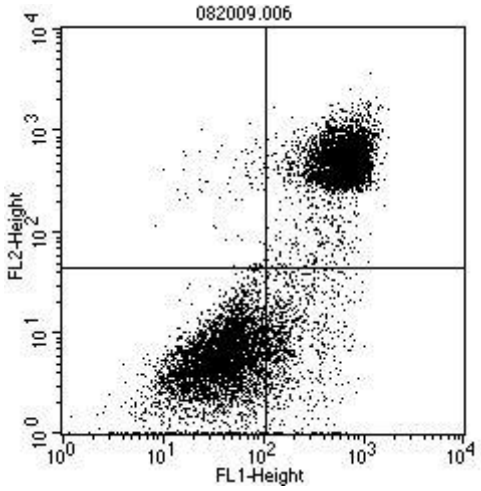

Figure 4.3 Static BAEC– AnnexinV/PI flow cytometry

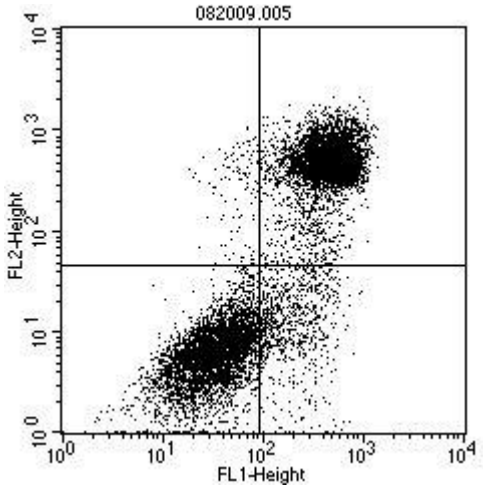

Figure 4.4 Static + TNF-α – AnnexinV/PI flow cytometry

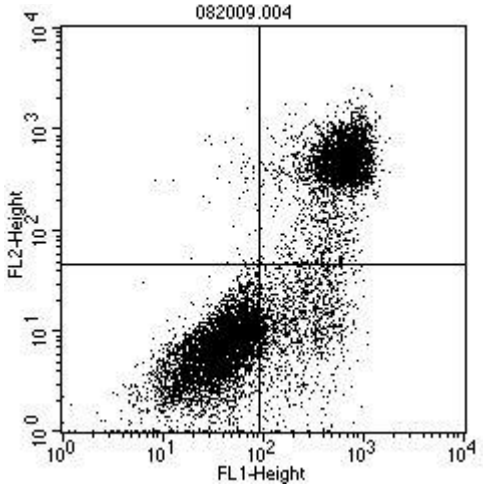

Figure 4.5 6hr SS + TNF-α – AnnexinV/PI flow cytometry

The flow cytometry results were averaged based on the four quadrants cells fell into during analysis. All experiments were repeated on three separate occasions, n = 3. The flow cytometry data is displayed in Figure 4.6.

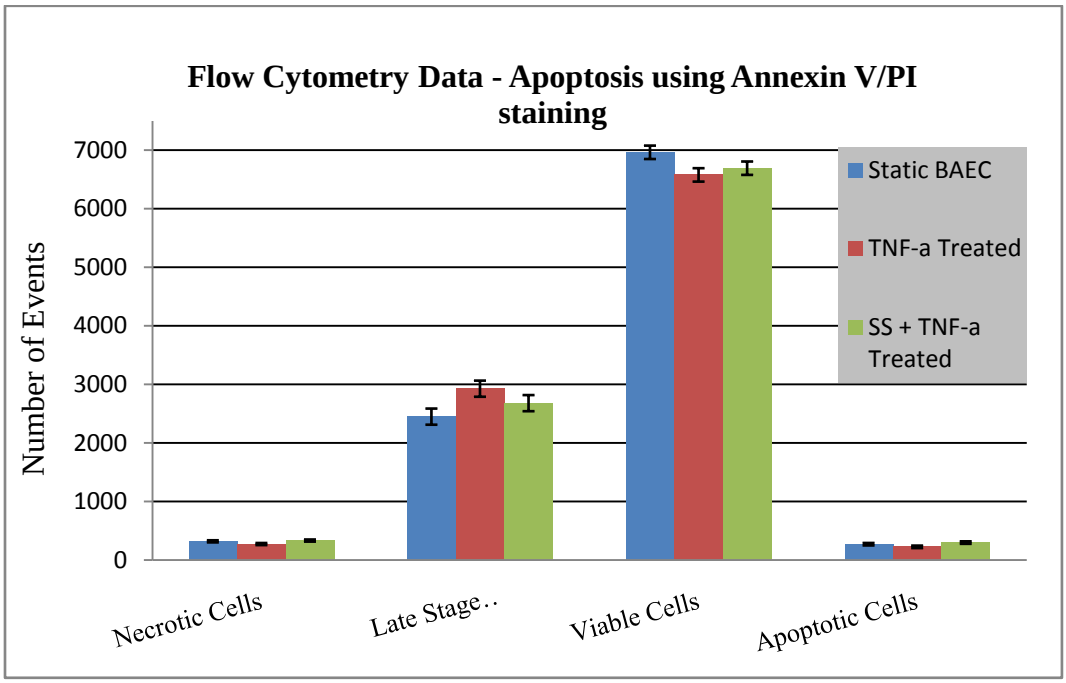

Figure 4.6 Apoptosis results using Annexin V and flow cytometry

TNF-α treated cells showed the highest amount of late stage apoptotic and necrotic cells, as well as the least amount of viable cells. Cells exposed to shear stress and TNF-α displayed a higher number of viable cells. We expected shearing to reduce TNF-α induced apoptosis, however, the increased apoptotic cells in the sheared condition could be due to stress from manipulation of cells in flow chamber. Annexin V is a cell surface marker and sensitive toward cell treatments. Therefore, cell treatments and experimental handling of sheared cells could have induced cell death, skewing results. More experiments were needed to optimize the assay, to analyze apoptosis in the study.

4.3.2 TUNEL - Fluorescence Microscopy

As previously mention, three different images were taken at each site: a cell phase image, used to find confluent cell areas, a GFP image, showing the TUNEL positive cells, and a DAPI image, displaying all of the cell nuclei for a count of the total number of cells. In Figure 4.7, all three images, taken at one location, are presented individually.

When imaging the sample slides, the cell phase setting was used to scan the glass slide for a confluent section, due to the possibility of cell loss in the shearing or staining subsequent steps. GFP and DAPI images were taken at the same location as the cell phase image. Images were taken from sites all across the slide to obtain a collective representation of the endothelial cell response in each experimental setup. Figure 4.7 are sample cell images taken at one specific site, with a scale bar equal to 50 microns.

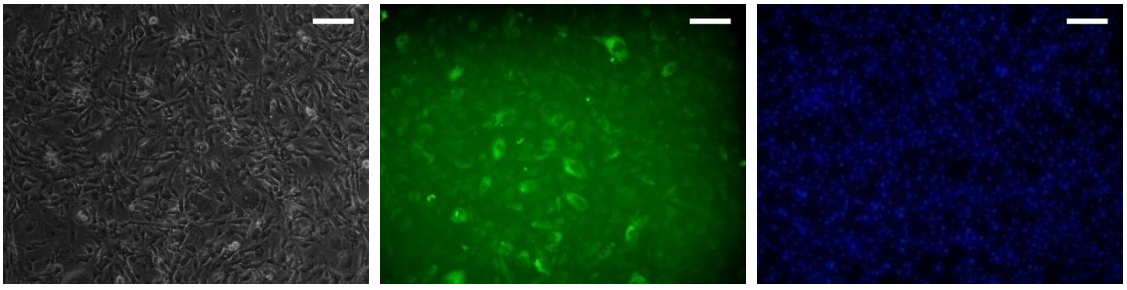

(A) (B) (C)

Figure 4.7 Fluorescence microscopy images at the same site; (A) Cell phase image, (B) GFP image, (C) DAPI image

After imaging all of the samples, the individual pictures were analyzed by Image Pro software. The GFP images were analyzed to quantify the total number of TUNEL positive cells in that population. In order to separate positive and negative, a fluorescence threshold was set for each image, allowing for Image Pro quantitative analysis of the positive cell number. Likewise, the DAPI image was examined and all of the nuclei were cumulated for a total cell count. Once both images were quantified, the percent positive was calculated using:

$$\% \text{ Apoptotic cells} = (\text{TUNEL positive cell number} / \text{total cell count}) * 100 \quad \text{Eq. 4.1}$$

In Figures 4.8 – 4.11, representative GFP images for each experiment condition are shown. As seen in the images, the control cells, without TNF-α or shear, display the least amount of TUNEL positive fluorescence, while the static + TNF-α without shear, display the most activity. Meanwhile, the sheared samples, introduced to TNF-α, have more TUNEL positive fluorescence, but a significantly smaller amount compared to the static + TNF-α sample. All of the images were ultimately quantified to verify the

qualitative image difference in the amount of apoptotic cells for each population. As shown in Figures 4.8 – 4.11, a sample image from each cell condition is displayed, including a scale bar equal to 50 microns.

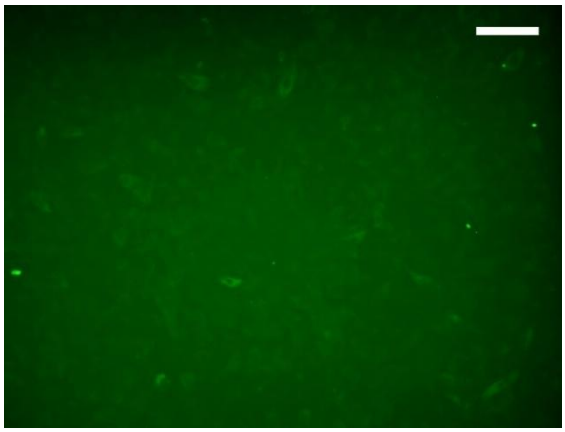

Figure 4.8 Control BAEC

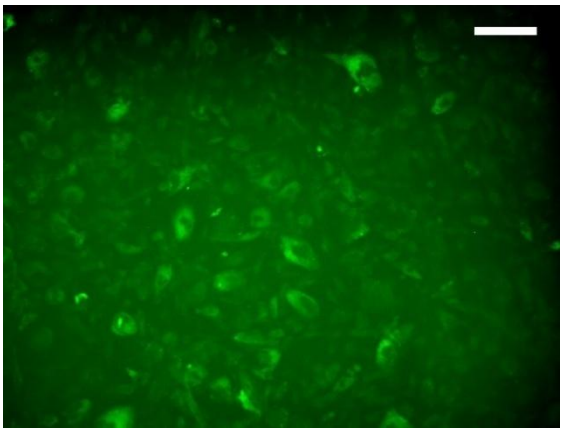

Figure 4.9 Static + TNF-α

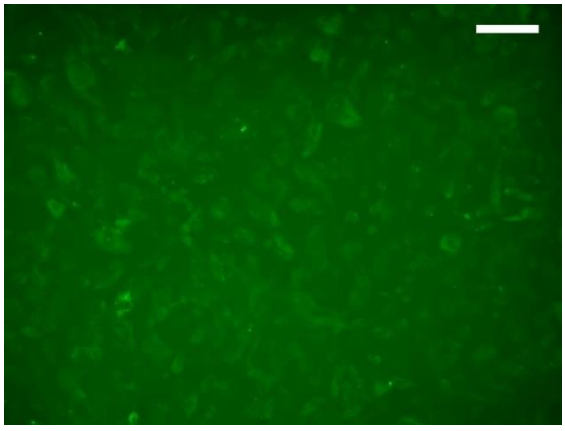

Figure 4.10 6hr SS + TNF-α

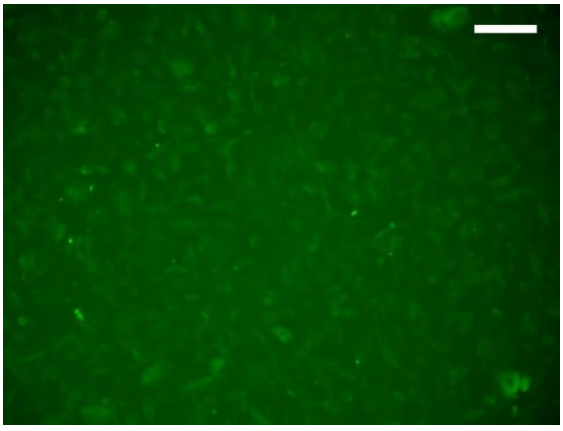

Figure 4.11 Pre-Sheared + TNF-α

After calculating all of the sample's population percentages, an average percent of apoptotic cells was determined for each representative experimental condition. All of the previously mentioned apoptotic experiments were repeated. In addition, 10 to 12 images were taken from each relative experiment, in an effort to gain complete understanding of the actual cell responses in each experiment.

After obtaining the average percent of apoptotic cells for each case, the experiments were analyzed in comparison plots. Figures 4.12 – 4.15 show the representative excel plots for each specific apoptosis experiment, along with the respective percent population of apoptotic cells per sample set.

Figure 4.12 shows the average population of apoptotic data from the first 6hr sheared subset. For statistical significance calculations, (*) represent p-values less than 0.05, as described in Section 3.3.1.5. As seen in the figure, the Static + TNF-α increased apoptosis activation by almost 2 fold compared to the control expression. Also, although the cell samples were incubated with TNF-α for the same length of time, the 6hr shear stress sample displayed a significantly smaller percent of apoptotic cells.

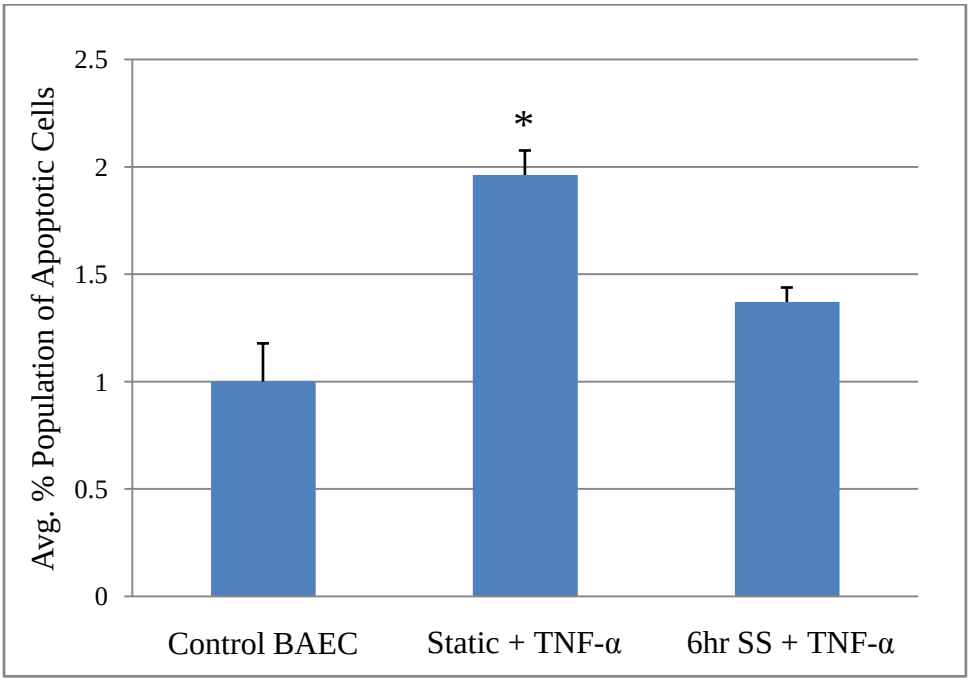

Figure 4.12 TUNEL apoptosis assay - 6hr SS vs. Static in TNF-α – run 1

Figure 4.13 shows the apoptosis results for the second 6hr sheared subset. The plot data exhibits a significant comparable difference to previous data between the static and 6 hr samples, regardless of the same incubation periods with TNF-α. These results lead to an assumed direct shear-induced affect on the TNF-α apoptosis cascade.

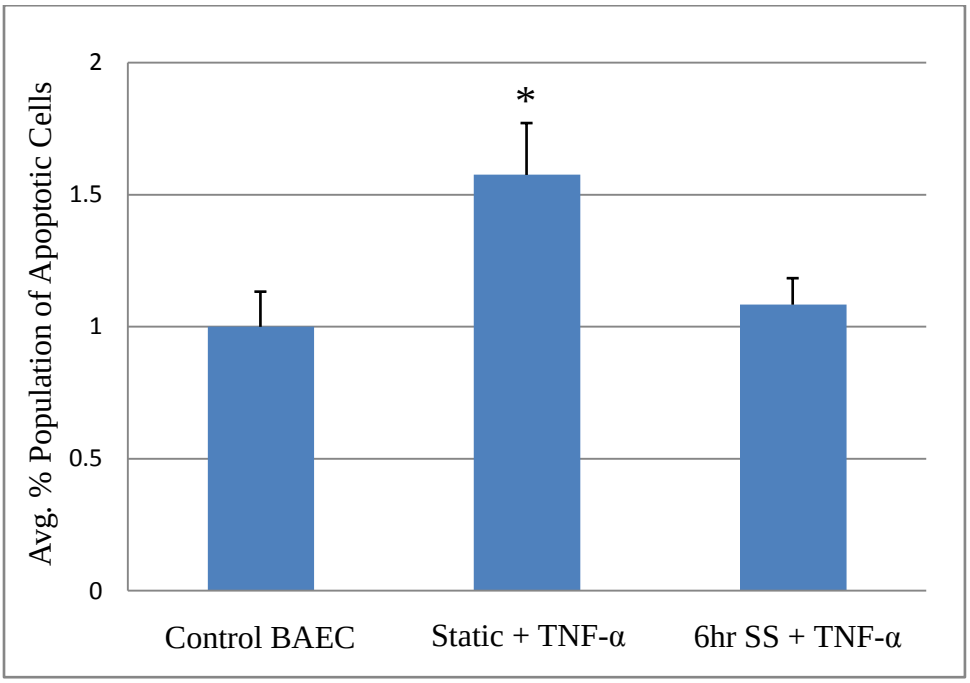

Figure 4.13 TUNEL apoptosis assay - 6hr SS vs. Static in TNF-α – run 2

Figures 4.14 and 4.15 represent both fluorescence microscopy trial results involving the static versus pre-sheared cell experiments. The pre-sheared cells were exposed to 1 hour of shear stress before the overnight incubation with TNF-α. The static cells also began TNF-α incubation at the same time. The pre-sheared cells exhibited a small effect to the TNF-α activation, and apoptosis levels were similar to the control endothelial cells. The TNF-α activated static cells displayed approximately twice as much apoptosis activity as both the other cell samples.

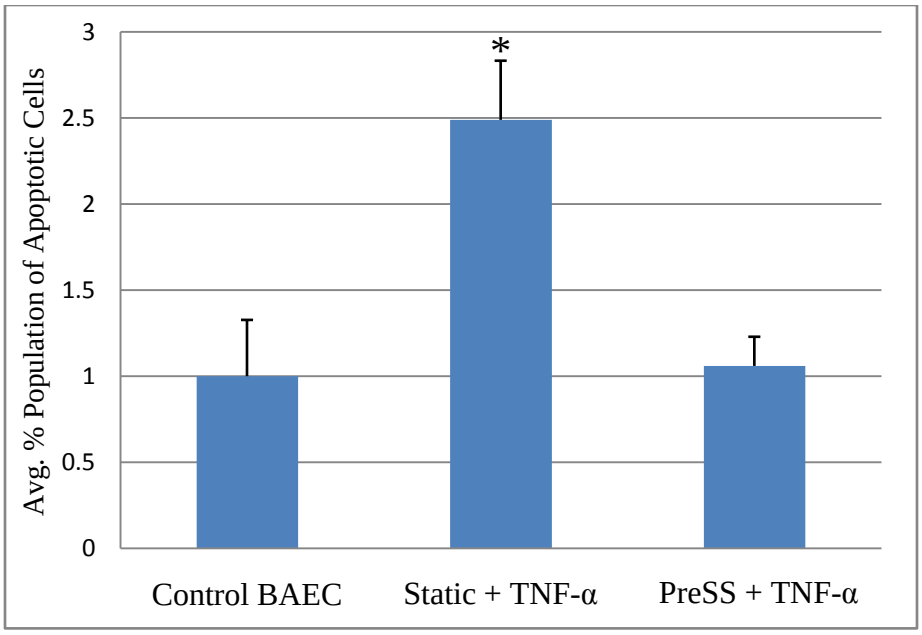

Figure 4.14 TUNEL apoptosis assay – Pre-sheared vs. Static – post shearing addition of TNF-α – run 1

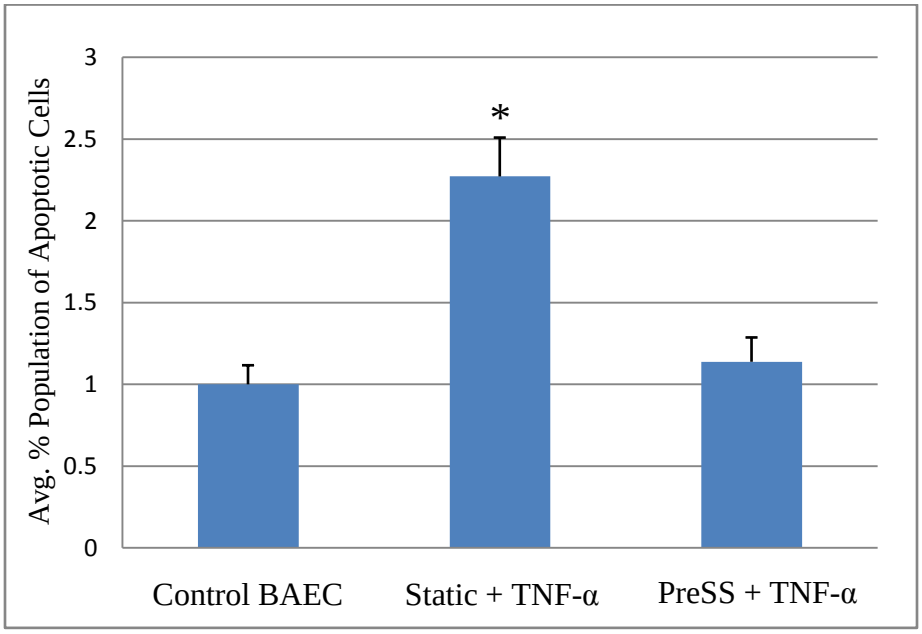

Figure 4.15 TUNEL apoptosis assay – Pre-sheared vs. Static – post shearing addition of TNF-α – run 2

4.3.3 TUNEL - Flow Cytometry

In order to verify the TUNEL fluorescence microscopy results, the static versus shear TUNEL experiments were repeated and analyzed using flow cytometry. The control cell sample was run in the flow cytometry to set the quadrant separation. Once the fluorescence threshold was determined, the static and sheared cells were analyzed. Cells showing fluorescence intensity higher than the threshold are TUNEL positive, considered apoptotic. The cytometry plots are shown in Figures 4.16 – 4.19.

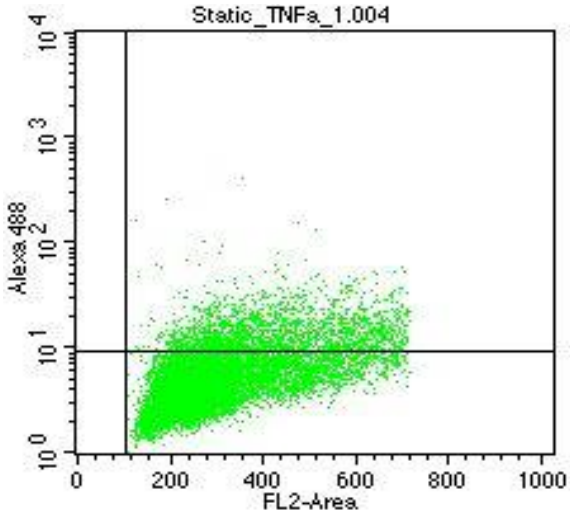

Figure 4.16 Static + TNF-α – TUNEL flow cytometry

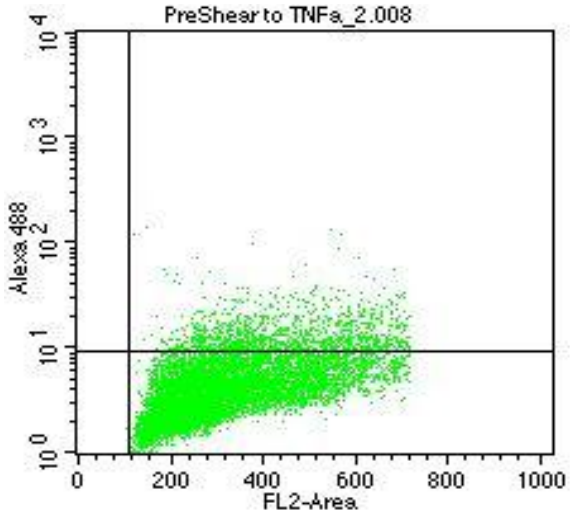

Figure 4.17 Pre-Sheared then TNF-α – TUNEL flow cytometry

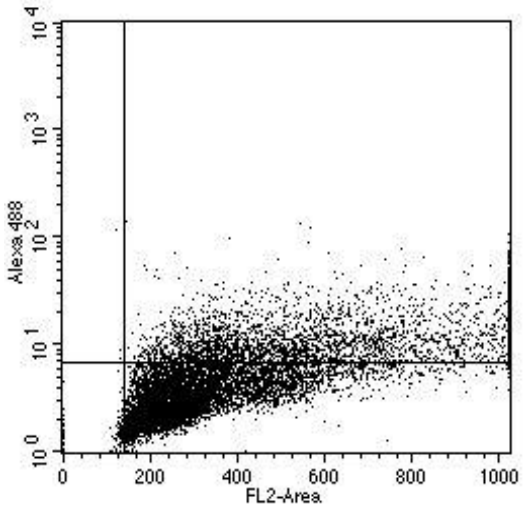

Figure 4.18 6hr Sheared + TNF-α – TUNEL flow cytometry

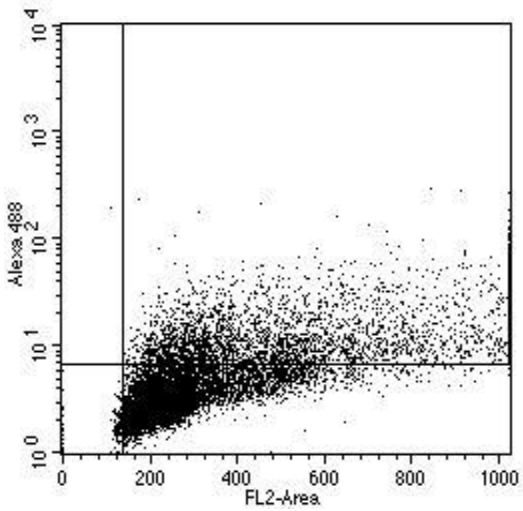

Figure 4.19 Static + TNF-α – TUNEL flow cytometry

Once the cellular events are categorized, the average percent populations of apoptotic cells were quantified and are displayed in Figures 4.20 and 4.21. The apoptotic population percents are expressed according to the percent cell populations of the sample. For statistical significance calculations, (*) represent p values less than 0.05.

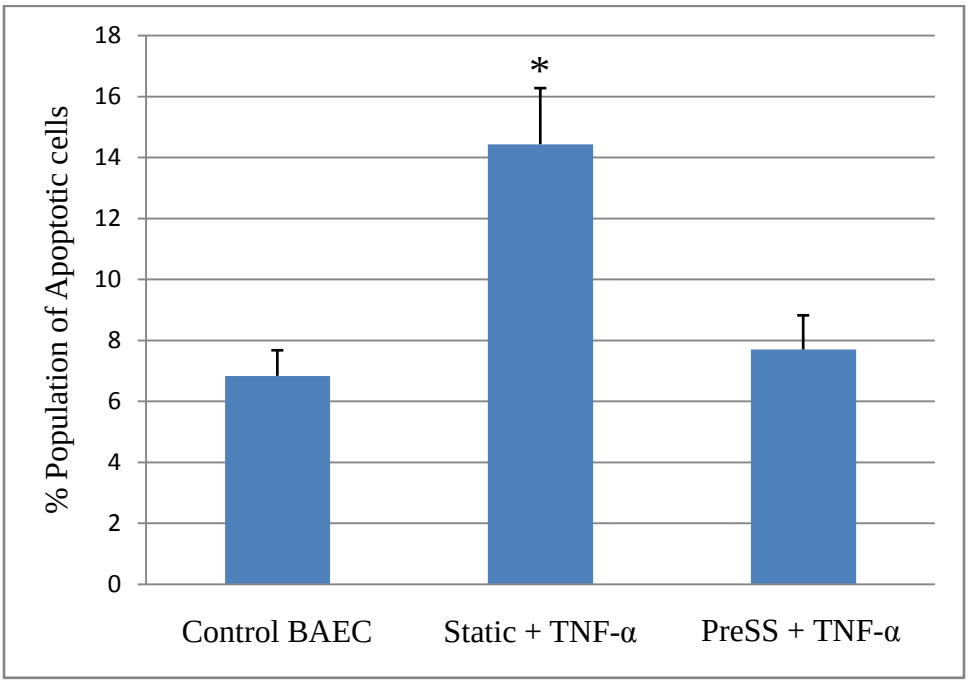

Figure 4.20 Flow cytometry – TUNEL analysis – Pre-sheared vs. Static BAEC - Post shearing addition of TNF-α

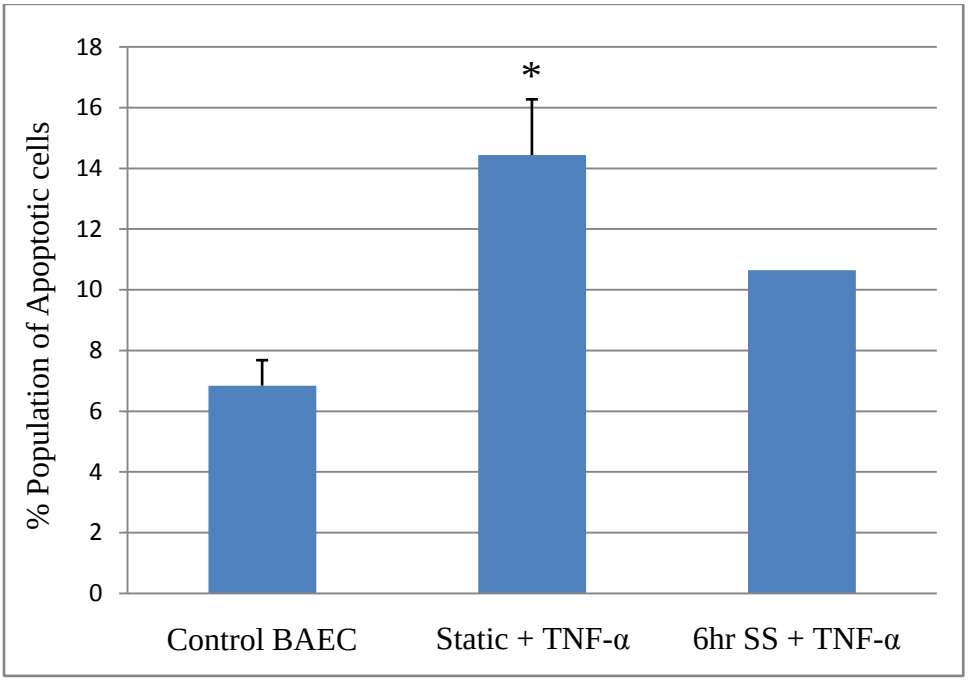

Figure 4.21 Flow cytometry – TUNEL analysis – 6hr SS vs. Static BAEC

As seen from Figures 4.20 and 4.21, the TUNEL flow cytometry data showed a closely related end result, when compared with the microscopy data in Figures 4.12 – 4.15, respectively. The Static + TNF-α samples show at least a two fold increase in apoptotic activity as opposed to the control cells. Also, both sheared samples displayed a decreased activation of apoptosis when compared with the TNF-α activated static cell samples.

4.4 Discussion

From the apoptosis assay results, one can see that treating cells with TNF-α under static conditions had increased apoptosis activity by at least two-fold, when compared to the control cells. Even with the same TNF-α incubation times, both sets of sheared cells showed less affected to cytokine and apoptosis activation.

On the other hand, there was a difference between the pre-sheared and post-sheared TNF-α activation. The pre-sheared cells exhibited very little effect from the TNF-α activation, and were approximately comparable to the control BAEC apoptosis levels. The pre-shearing exposure seemed to up-regulate anti-apoptotic expression, negating the effects of cytokine activation. The 6hr sheared cells were exposed to shear for a longer time period, possibly incorporating homeostatic cell turnover, necessary for maintaining tissue integrity and function. As shown, both pre-shearing and shearing cells with TNF-α activation were observed to down-regulate apoptosis response in endothelial cells. This data suggests that the laminar shear exposure seems to play part in an anti-apoptotic, protective pathway in antagonizing the TNF-α induced death cascade, and that short time pre-shearing of cells is as potent as simultaneous shearing of cells under TNF-α activation, in reducing apoptosis.

5. CONCLUSIONS AND RECOMMENDATIONS

5.1 Conclusions

Factors, such as cell apoptosis and cell structural remodeling, can create instability in arterial plaque build-up. Further arterial lesion disruptions could lead to a rupture in the blood vessel wall, allowing for thrombosis formation and additional accumulation at the damage site. The affects of shear stress on cell turnover could play a role in up-regulating certain factors that influence atherosclerosis progression.

DAPK, which is shown to be up-regulated in arterial plaque, is a factor in apoptotic, programmed cell death, activities. Additionally, shear stress due to flow activates certain cellular signaling cascades, thought to affect cell turnover and cell wall permeability, and influencing apoptosis.

Due to various lengths of exposed shear stress, a DAPK protein expression profile was developed using immuno-precipitation blotting. With applied shear, DAPK increases overall protein expression, while decreasing phosphorylated DAPK as it becomes activated. The gene expression data provides a DAPK mRNA activation pattern that develops the relationship between shear stress induced protein and mRNA expression. The DAPK mRNA activation with short shear time (2 and 4 hrs) correlates with the increase in DAPK protein expression. Yet, the mRNA activation returns to basal level after an 8 hr shear exposure. To clearly understand DAPK expression, extended shear exposure experiments are needed to understand the subsequent pattern of expression and long-term shearing responses

Apoptosis assay optimization was established to further delineate the role of DAPK in shear stress induced effects on endothelial apoptosis. The final objective was to deduce a connection between the effects of applied shear on apoptosis and the DAPK gene expression profiles. Overall, the apoptosis activity influenced by shear further exhibits a possible connection between shear stress and anti-apoptotic activities. Yet in relation to DAPK, the shear stress ultimately decreases overall apoptosis, while DAPK is increased due to shearing. Therefore, DAPK might have a role in other possible mechano-transduction cascades, when endothelial cells are exposed to constant shear. Further apoptosis research is needed to investigate the other possible involvements of DAPK when cells are sheared.

5.2 Future Research

In order to further develop the DAPK gene expression profile, protein expression needs to be examined using longer than 8 hours of applied shear. The extended shear could lead to a possible temporal expression pattern, as seen in the mRNA plot. Likewise, the DAPK mRNA profile could be expanded to see if the expression recovers or remains in a down-regulated state, depleting overall DAPK protein expression in long term shear situations.

In response to shear, overall DAPK expression is up-regulated, while there is an overall decline in apoptosis events. Due to these results, DAPK may have a different role under shear stress, possibly in cytoskeletal responses rather than apoptosis cascades.

Future research will further examine the role of DAPK in affecting multiple endothelial cell functions under shear stress. For instance, studies will look at DAPK influences in cytoskeleton and cell motility/alignment. Similarly, studies could examine the possible activation of other phosphorylation sites, which may negate apoptotic pathways or stimulate anti-apoptotic genes.

The functional roles of endothelial DAPK in response to shear stress will also be examined using siRNA targeting DAPK expression, as well as over expression of DAP-kinase within the cells. These results will help determine the potential role of DAPK in the progression of atherosclerosis, and aid in the development of novel approaches both in the prevention and treatment of atherosclerosis.

LIST OF REFERENCES

LIST OF REFERENCES

[1] Alberts et al. (2002). *Molecular Biology of the Cell,* Fourth edition. New York, Garland Science.

[2] Stijn A.I. (2009). "Anatomy overview of a human artery." http://commons.wikimedia.org/wiki/File:Anatomy_artery.png. Last accessed April 2010.

[3] Hahn, C., Schwartz, M. (2009). "Mechanotransduction in vascular physiology and atherogenesis." *Nature Reviews Molecular Cell Biology* 10, 53-62 doi:10.1038/nrm2596.

[4] Arab, A., K. Kuemmerer, et al. (2008). "Oxygenated perfluorochemicals improve cell survival during reoxygenation by pacifying mitochondrial activity." *J Pharmacol Exp Ther* 325(2): 417-424.

[5] Li, Y. S., J. H. Haga, et al. (2005). "Molecular basis of the effects of shear stress on vascular endothelial cells." *J Biomech* **38**(10): 1949-1971.

[6] Anderson, J. W. and T. L. Floore (1990). "Lipoproteins and diet in the pathogenesis of atherosclerosis." *Adv Exp Med Biol* **273**: 245-258.

[7] Maton et al. (1993). *Human Biology and Health*. Upper Saddle River, N.J., Prentice Hall.

[8] Malek, A. M., S. L. Alper, et al. (1999). "Hemodynamic shear stress and its role in atherosclerosis." *JAMA* **282**(21): 2035-2042.

[9] Ellis, J. T., D. L. Kilpatrick, et al. (2005). "Therapy considerations in drug-eluting stents." *Crit Rev Ther Drug Carrier Syst* **22**(1): 1-25.

[10] Berliner, J. A., M. Navab, et al. (1995). "Atherosclerosis: basic mechanisms. Oxidation, inflammation, and genetics." *Circulation* **91**(9): 2488-2496.

[11] Mayo Clinic. "Development of Atherosclerosis." https://www.bcbsri.com/BCBSRIWeb/images/mayo_popup/Developmentofatherosclerosis.jsp. Last accessed January 2010.

[12] Glaudemans, A. W., R. H. Slart, et al. (2010). "Molecular imaging in atherosclerosis." *Eur J Nucl Med Mol Imaging*.

[13] NIH. MedLine Plus. Dugdale, D. (2006). "Atherosclerosis." http://www.nlm.nih.gov/medlineplus/ency/imagepages/18018.htm. Last accessed March 2010.

[14] Amir, S. and C. J. Binder (2010). "Experimental immunotherapeutic approaches for atherosclerosis." *Clin Immunol* **134**(1): 66-79.

[15] Xu, Q. (2009). "Disturbed flow-enhanced endothelial turnover in atherosclerosis." *Trends Cardiovasc Med* **19**(6): 191-195.

[16] Anderson, N. G., J. L. Maller, et al. (1990). "Requirement for integration of signals from two distinct phosphorylation pathways for activation of MAP kinase." *Nature* **343**(6259): 651-653.

[17] Keranen, L. M., E. M. Dutil, et al. (1995). "Protein kinase C is regulated in vivo by three functionally distinct phosphorylations." *Curr Biol* **5**(12): 1394-1403.

[18] Pawson, T. and P. Nash (2000). "Protein-protein interactions define specificity in signal transduction." *Genes Dev* **14**(9): 1027-1047.

[19] Bialik, S., A. R. Bresnick, et al. (2004). "DAP-kinase-mediated morphological changes are localization dependent and involve myosin-II phosphorylation." *Cell Death Differ* **11**(6): 631-644.

[20] Kuo, J. C., J. R. Lin, et al. (2003). "Uncoordinated regulation of stress fibers and focal adhesions by DAP kinase." *J Cell Sci* **116**(Pt 23): 4777-4790.

[21] Kuo, J. C., W. J. Wang, et al. (2006). "The tumor suppressor DAPK inhibits cell motility by blocking the integrin-mediated polarity pathway." *J Cell Biol* **172**(4): 619-631.

[22] Cohen, O., E. Feinstein, et al. (1997). "DAP-kinase is a Ca2+/calmodulin-dependent, cytoskeletal-associated protein kinase, with cell death-inducing functions that depend on its catalytic activity." *EMBO J* **16**(5): 998-1008.

[23] Kimchi, A. (1998). "DAP genes: novel apoptotic genes isolated by a functional approach to gene cloning." *Biochim Biophys Acta* **1377**(2): F13-33.

[24] Cohen, O., B. Inbal, et al. (1999). "DAP-kinase participates in TNF-alpha and Fas-induced apoptosis and its function requires the death domain." *J Cell Biol* **146**(1): 141-148.

[25] Anjum, R., P. P. Roux, et al. (2005). "The tumor suppressor DAP kinase is a target of RSK-mediated survival signaling." *Curr Biol* **15**(19): 1762-1767.

[26] Shohat, G., G. Shani, et al. (2002). "The DAP-kinase family of proteins: study of a novel group of calcium-regulated death-promoting kinases." *Biochim Biophys Acta* **1600**(1-2): 45-50.

[27] Chen, C. H., W. J. Wang, et al. (2005). "Bidirectional signals transduced by DAPK-ERK interaction promote the apoptotic effect of DAPK." *EMBO J* **24**(2): 294-304.

[28] Wang, W. J., J. C. Kuo, et al. (2007). "The tumor suppressor DAPK is reciprocally regulated by tyrosine kinase Src and phosphatase LAR." *Mol Cell* **27**(5): 701-716.

[29] Hupp, T. R. (2010). "Death-associated protein kinase (DAPK) and signal transduction." *FEBS J* **277**(1): 47.

[30] Raveh, T., G. Droguett, et al. (2001). "DAP kinase activates a p19ARF/p53-mediated apoptotic checkpoint to suppress oncogenic transformation." *Nat Cell Biol* **3**(1): 1-7.

[31] Shohat, G., T. Spivak-Kroizman, et al. (2002). "The regulation of death-associated protein (DAP) kinase in apoptosis." *Eur Cytokine Netw* **13**(4): 398-400.

[32] Bovellan, M., M. Fritzsche, et al. (2010). "Death-associated protein kinase (DAPK) and signal transduction: blebbing in programmed cell death." *FEBS J* **277**(1): 58-65.

[33] Davies, P. F., A. Remuzzi, et al. (1986). "Turbulent fluid shear stress induces vascular endothelial cell turnover in vitro." *Proc Natl Acad Sci U S A* **83**(7): 2114-2117.

[34] Martinet, W., D. M. Schrijvers, et al. (2002). "Gene expression profiling of apoptosis-related genes in human atherosclerosis: upregulation of death-associated protein kinase." *Arterioscler Thromb Vasc Biol* **22**(12): 2023-2029.

[35] Braddock, M., J. L. Schwachtgen, et al. (1998). "Fluid Shear Stress Modulation of Gene Expression in Endothelial Cells." *News Physiol Sci* **13**: 241-24.

[36] Chiu, J. J., P. L. Lee, et al. (2005). "Shear stress regulates gene expression in vascular endothelial cells in response to tumor necrosis factor-alpha: a study of the transcription profile with complementary DNA microarray." *J Biomed Sci* **12**(3): 481-502.

[37] Fox, R., McDonald, A., and Pritchard, P. (2003). *Introduction to Fluid Mechanics*, Sixth ed. New York, John Wiley and Sons.

[38] Papavassiliou, A. G. (1994). "Preservation of protein phosphoryl groups in immunoprecipitation assays." *J Immunol Methods* **170**(1): 67-73.

[39] Penna A, Cahalan M. (2007). "Western Blotting Using the Invitrogen NuPage Novex Bis Tris MiniGels." *JoVE*. doi: 10.3791/264, http://www.jove.com/index/details.stp?id=264. Last accessed April 2010.

[40] Hawkes, W. C., T. T. Wang, et al. (2009). "Selenoprotein W modulates control of cell cycle entry." *Biol Trace Elem Res* **131**(3): 229-244.

[41] Applied Biosystems. (2006). "High Capacity cDNA Reverse Transcription Kit." http://www3.appliedbiosystems.com/cms/groups/mcb_marketing/documents/generaldocuments/cms_039876.pdf. Last accessed March 2010.

[42] Hoffmann, A. C., J. T. Kaifi, et al. (2009). "Lack of prognostic significance of serum DNA methylation of DAPK, MGMT, and GSTPI in patients with non-small cell lung cancer." *J Surg Oncol* **100**(5): 414-417.

[43] Board of Reagents, Univ. of Wisconsin. (2007). "Primer binding plot." http://bioweb.uwlax.edu/GenWeb/Molecular/Seq_Anal/Primer_Design/primer_design.htm#designrules. Last accessed February 2010.

[44] Rozen, S., Skaletsky, H. (2000). "Primer3 on the WWW for general users and for biologist programmers." *Bioinformatics Methods and Protocols: Methods in Molecular Biology*. Humana Press, Totowa, NJ, pp 365-386.

[45] Richards, G. P., M. A. Watson, et al. (2004). "A SYBR green, real-time RT-PCR method to detect and quantitate Norwalk virus in stools." *J Virol Methods* **116**(1): 63-70.

[46] Hunt, M., Univ. of South Carolina, "Real-Time PCR." http://pathmicro.med.sc.edu/pcr/realtime-home.htm. Last accessed March 2010.

[47] Garin, G., J. Abe, et al. (2007). "Flow antagonizes TNF-alpha signaling in endothelial cells by inhibiting caspase-dependent PKC zeta processing." *Circ Res* **101**(1): 97-105.

[48] Koopman, G., C. P. Reutelingsperger, et al. (1994). "Annexin V for flow cytometric detection of phosphatidylserine expression on B cells undergoing apoptosis." *Blood* **84**(5): 1415-1420.

[49] BD Biosciences. (2002). "BD CellQuest Pro Acquisition Tutorial." Becton, Dickinson and Company. http://facs.stanford.edu/sff/doc/cellquestprouser guide.pdf. Last accessed March 2010.

[50] Heatwole, V., et al. (2000). "TUNEL Assay for Apoptotic Cells." *Methods in Molecular Biology*, Vol. 115: Immunocytochemical Methods and Protocols.